Aksoy *New Zealand Journal of Forestry Science* (2024) 54:20
https://doi.org/10.33494/nzjfs542024x328x
E-ISSN: 1179-5395
published on-line: 15/12/2024

RESEARCH ARTICLE Open Access

New Zealand Journal of Forestry Science

Evaluation of forest areas and land use/cover (LULC) changes with a combination of remote sensing, intensity analysis and CA-Markov modelling

Hasan Aksoy

Sinop University, Vocational School of Ayancık, Department of Forestry, Program of Forestry and Forest Products, Sinop, Türkiye

*Corresponding author: haksoy@sinop.edu.tr

(Received for publication 20 August 2023; accepted in revised form 25 November 2024)
Editor: Euan G. Mason

Abstract

Background: Land use and land cover change (LULC) is crucial for maintaining the integrity of ecosystems' structure and function, and thus regular measurement and monitoring of LULC are necessary.

Methods: In this study, the temporal and spatial changes in forest areas and land cover in the province of Sinop, located in the north of Turkey, were analysed by intensity analysis for two 10-year periods from 2002-2012 to 2022, and 2032 and 2042 forecast LULC maps were generated using the cellular automata CA-Markov model. In the study, datasets were prepared using forest type maps and Landsat images, and the images were classified using various classification techniques.

Results: The results indicated that forest areas increased by 23% (37,823.38 ha) from 2002 to 2022, with the mixed forest category showing a decrease of 22% (12,245.43 ha) within this. In non-forest areas, a significant increase of 72% was observed in the settlement category, while a decrease of 63% was noted in the agricultural category. According to the intensity analysis, the rate of change in LULC is faster from 2002 to 2012 than from 2012 to 2022. In both periods, the settlement and agricultural categories have predominantly targeted each other's losses. According to the simulation results of land use/cover from 2022 to 2042, a 0.50% increase in total forest area, a 2.87% increase in settlements, and a decrease of 2.65% and 0.71% in agriculture and water classes, respectively, are anticipated.

Conclusions: The overall results suggest that it can contribute to setting an appropriate development goal, especially for forest planners and policymakers, to regulate land use changes to achieve higher carbon stocks and maintain balance in global climate scenarios.

Keywords: LULC; Satellite images; GIS; Forest cover changes; Intensity analysis.

Introduction

Humanity has explored and benefited from various ecosystems since its existence, leading to significant changes in land-use/land-cover change (LULC) in different scales and forms up to the present day (Bewket & Abebe 2013; Hishe et al. 2020). Land change is widely recognized as a major factor influencing the world's ecosystems and climate (Pellikka et al. 2018; Das et al. 2021). Land use and land cover change are estimated to have caused 12.5% of all anthropogenic carbon dioxide emissions from 1990 to 2010 (Houghton et al. 2012; Das et al. 2021). Terrestrial ecosystems are the most important ecosystems in terms of carbon sequestration capacity. In particular, the sustainability of the services provided by terrestrial forest ecosystems is very important. Environmental problems, especially global warming, threaten the lives of living things, and their effects are felt intensely all over the world. Land use and land cover changes (LULC) are one of the most current and worrying of these problems (Dewan & Yamaguchi 2009; Halmy et al. 2015; Zheng et al. 2015; Karimi et al. 2018), which are caused by the mutual interaction of natural processes and human influence (Agarwal 2002; Zadbagher et al. 2018). Many factors influence the LULC process, including ecological, socioeconomic, and political conditions, land planning systems, and

environmental impacts (Mayes et al. 2014; Nasiri et al. 2019). LULC changes are often linked to human intervention (Achmad et al. 2015), agricultural needs (Santer et al. 2000; Cammerer et al. 2013; Li et al. 2013; John et al. 2020), natural disasters (Dubovyk et al. 2011), economic and urban developments (Khan et al. 2015; Rimal et al. 2019) due to population growth. Uncontrolled and unplanned LULC change can lead to many negative consequences such as ecosystem integrity, natural resource consumption, reduction of biological diversity, extinction of species, and climate change (López-Moreno et al. 2014; Peralta-Rivero et al. 2014; Huang et al. 2015; Nasiri et al. 2019). People are migrating from the countryside to the city due to the increased availability of opportunities and facilities such as employment, education, health, and other recreational activities (Hasan et al. 2020). Therefore, especially developing countries are faced with habitat fragmentation, conversion of forests to agriculture and urban structures, and deforestation (Sahana et al. 2016; Ghosh & Porchelvan 2017; Hermhuk et al. 2020). To determine where, when, and at what rate LULC change occurs, these changes need to be continuously monitored and evaluated at different spatial and temporal scales (Mengistu & Salami 2007; Kumar et al. 2016; Singh et al. 2022). So, regional mapping of LULC, detecting the rate and transition between variables, and revealing future changes is essential for more sustainable land use (Mengistu & Salami 2007; Kafi et al. 2014; Alipbeki et al. 2020). All the topics and information mentioned above illustrate the importance of rapidly and reliably delineating LULC.

The fact that LULC is difficult to monitor with traditional methods and data acquisition has led researchers to different data sources and using remote sensing data as an alternative; the most effective data source. The integration of remote sensing (RS) and geographic information systems (GIS) is widely used in different parts of the world to investigate the extent of natural ecosystems and resources, their changes over time, and the speed of change (Dong et al. 2009; Santillan et al. 2011; Mallupattu & Sreenivasula Reddy 2013; Liu et al. 2014; Yagoub & Al Bizreh 2014; Abino et al. 2015). RS and GIS are recognised as some of the most effective tools for monitoring LULC (Deep & Saklani 2014; John et al. 2020). In recent years, various spatial models have been developed to make it easier to study, model, and manage the LULC transformation process. Such models provide flexible and innovative possibilities that simplify the complex web of LULC transformations, contributing to informed decision-making and effective land management (Parker et al. 2003; Rubio et al. 2012; Aksoy & Kaptan 2021). Various modelling tools and techniques are used to spatially study and analyse the LULC process and predict future LULC change. The most widely used of these is the Cellular Automaton (CA Markov) chain (Isik et al. 2013; Basse et al. 2014; Qiang & Lam 2015; Nasiri et al. 2019). CA Markov is a statistical tool that uses a neighbourhood-based transition probability matrix in the spatial algorithm (Nouri et al. 2014). It is generally used to analyse losses and gains as percentages and probabilities of each type of land use that transforms within a certain period (Huang et al. 2008).

In recent years, many studies have been reported in the literature for the detection of LULC with RS data. Beroho et al. (2023) generated future land use/land cover (LULC) scenarios in the Mediterranean basin of Morocco using CA-Markov. Weslati et al. (2023) examined the modelling and evaluation of spatiotemporal changes in future land use change scenarios using remote sensing and the CA-Markov model in the Mellegue basin. Mathewos et al. (2022) created future predictions using the CA-Markov model by evaluating land use and land cover changes in the Rift Valley basin. Almirón et al. (2022), the impact of land use and climate change on species in South American forests. Researchers such as Gasirabo et al. (2023), Daba et al. (2022), Jana et al. (2022), and Khwarahm et al. (2021) have investigated future simulations using the CA-Markov model. To monitor and analyse LULC, it is necessary to calculate change matrices by overlaying the land use bases of different time points of a region. However, the direct interpretation of these matrices is insufficient to explain the processes and reasons for change (Huang et al. 2012, Kaptan 2021). Intensity analysis developed by Aldwaik and Pontius (2012) is used to eliminate or minimise this deficiency and to better interpret the processes and causes of changes in land use classes. Intensity analysis, which has become popular recently, is also frequently used by researchers to interpret the net changes between land classes.

The importance of assessing and monitoring LULC has focused Turkish researchers on this topic. However, many studies conducted in our country have focused regionally on determining the areal changes in land use classes, which is the most well-known aspect of LULC change. Only a few studies have focused on understanding which land use classes influence or target changes in other land use classes during land-use transitions. In this study, it was aimed to determine the interactions of land use classes with each other and the rate of change by using intensity analysis and to create future land use class maps with the CA-Markov model. In the study, forest cover types maps of 2002, 2012, and 2022 and Landsat satellite images were used. The relevant dates were selected because digital forest type maps were used to determine the land use classes for the analysis. The overall aim was to investigate the land use/land cover (LULC) changes between 2002, 2012, and 2022 using intensity analysis and to predict land use classes for the years 2032-2042. Another objective of the study is to provide specific information for the management, planning, rehabilitation, and policy approaches of forests, which are one of the natural ecosystems in Turkey, by revealing which land use class each land use class has changed and has the potential to change by targeting which land use class and by developing future scenarios based on this. The outputs of the study provide invaluable information to conservation ecologists, urban planners, and decision-makers to protect the integrity of ecosystems, as well as a basis for future simulations, measures, and planning for the region.

Methods

Study area, satellite images and land use data

The study was carried out in the province of Sinop, located in the northernmost part of Turkey (Figure 1). The study area is located between 34° 10′ 26″ and 35° 30′ 06″ E longitude and, 42° 05′ 30′′ and 41° 20′ 30″ N latitude. The study area is bordered by Çorum in the south, Samsun in the east, and Kastamonu province in the west. The study area consists of a total area of 556,275.50 hectares (ha), with forests covering 66.41% (369,466.00 ha) of the study area. The *Pinus nigra*, *Pinus sylvestris*, *Fagus orientalis*, *Carpinus betulus*, *Abies nordmanniana*, *Quercus infectoria*, *Quercus frainetto*, *Quercus cerris*, *Quercus petraea*, *Quercus robur*, *Juniperus* sp., *Fraxinus excelsior*, *Ulmus* L., Sp. and *Populus tremula* are the most common tree species in the Sinop. Summers are warm in the study region, which has a Black Sea climate, while winters are cool. The mean annual precipitation is 685.7 mm, with the most precipitation in October and the least in May (GDF 2022).

Landsat satellite images constitute the general basis of the study. Landsat satellite images of the study area for the years 2002, 2012, and 2022 were obtained from the official page of the United States Geological Survey (USGS 2022). In the study, satellite images in the same season and without clouds (<10%) were preferred to perform the image classification process at the highest level of accuracy. The features of the satellite images used are given in Table 1.

In the study, reference data (regions of interest (ROIs)) for the classification (training) and accuracy assessment (testing) of Landsat images were created based on the digital forest types maps of the study area (2002, 2012, and 2022). 50% of the pixel-based regions of interest (ROI) for each land use class were used for classification (training) and 50% were used for accuracy (testing) evaluation. These maps were obtained from the Sinop Regional Directorate of Forestry. The main reason for choosing the dates in the study is that the forest type maps for the study area were updated and revised in those years. These maps are generated based on very-high-resolution digital optical images, and field surveys. During this process, each stand type (including non-forest LULCs) is first delineated on the 30-cm colour-infrared stereo aerial photographs taken by the General Command of Mapping of Turkey. Then, stand type codes are assigned to the delineated polygons with 3D visual inspection in the Turkish Forestry Service (GDF)'s headquarters office in Ankara. In the next step, draft stand-types maps are sent to the forest professionals who perform forest inventory surveys in respective PUs. The draft maps are spatially and thematically corrected after field observations and ground measurements conducted in hundreds of forest sample plots. Thus, the final stand-types maps are generated at the PU (landscape) level. These maps are periodically updated in Turkey as forest management plans are generally renewed at 10- or 20-year intervals (Aksoy & Kaptan, 2021). Six land use classes were determined on forest type maps and made

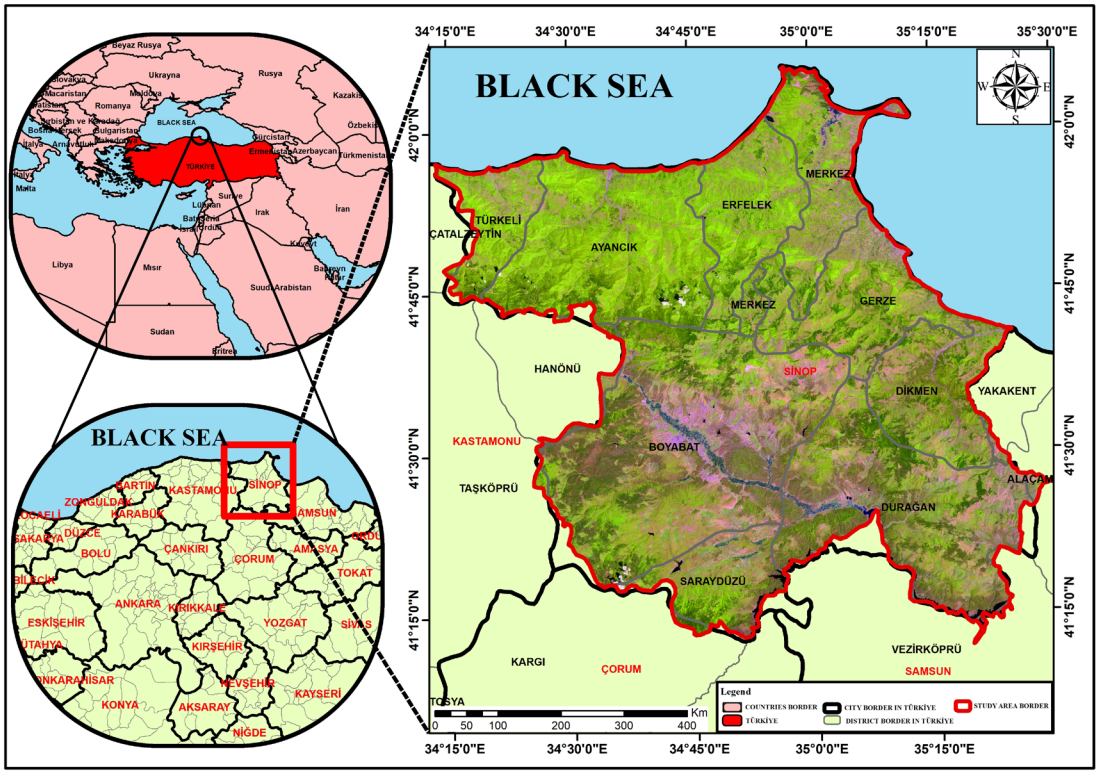

FIGURE 1: The location of the study area in the world and in Türkiye.

TABLE 1: Landsat satellite features (https://earthexplorer.usgs.gov/).

Satellite	Date Acquired	Path	Row	Spectral Range	Wavelength (µm)		Spatial Resolution (m)
					Landsat ETM	Landsat 8 OLI	
Landsat 7 ETM+	29.06.2002 28.06.2012	176	31	Band 1	0.45 – 0.51	0.43 – 0.45	30
				Band 2	0.53 – 0.61	0.45 – 0.51	30
Landsat 8 OLI/TIRS	01.09.2022			Band 3	0.63– 0.69	0.53 – 0.59	30
				Band 4	0.75 – 0.90	0.64 – 0.67	30
				Band 5	1.55 – 1.75	0.85 – 0.88	30
				Band 6	10.4 – 12.5	1.57 – 1.65	30
				Band 7	1.09 – 2.35	2.11 – 2.29	30
				Band 8	0.52 – 0.90	0.50 – 0.68	15

ready for analysis. The land use classes used in the study, along with their main and subcategories, are shown in Table 2.

General methodology of the study

In the study, Landsat-7 ETM + for 2002 and 2012, and Landsat-8 OLI images for 2022 were classified by supervised classification method, concerning forest type maps of the area. Maximum-likelihood classification (MLC), Support-vector machine (SVM), and Random-forest (RF) methods were used in the supervised classification process. ENVI version 5.3 software was used for classification and accuracy analysis. The Cellular Automata-Markov (CA-Markov) model has been constructed using transition probability matrices for the periods 2002-2012, 2012-2022, and 2002-2022, along with simulation maps for 2022, 2032, and 2042. The modelling accuracy was verified using Kappa statistics and F1-Score values, employing Regions of Interest (ROIs) prepared for the classification of the 2022 Land Use Land Cover (LULC) map. After checking the accuracy of the model, land use simulation maps of the study area were produced for the years 2032 and 2042. The general methodological flow of the study is shown in Figure 2.

Satellite image pre-processing and classification approaches

Atmospheric correction was applied to the Landsat satellite images used in the study. To distinguish land use classes with maximum accuracy, satellite images with 1% standard deviation geometric correction were made. In satellite images, some systematic errors may

TABLE 2: Land use classes.

	Class					
	Coniferous Forest (CF)	**Mixed Forest (MF)**	**Broad-leaved Forest (BLF)**	**Settlement (St)**	**Agriculture (Ag)**	**Water (Wt)**
Class Content	Pure Crimean pine	Scots pine & Nordmann's fir	Sycamore	City Centre	Cultivated Land	Lake
	Scots pine	Beech & Nordmann's fir	Oak	District Centre	Uncultivated Land	Barrage
	Maritime pine	Beech & Scots	Beech	Village Centre	Forest, Treeless	River
	Nordmann's fir	Nordmann's fir & Hornbeam	Hornbeam	Rural Settlement	Garden	
	Gall	Pure Crimean pine & Beech	Maple			
	Common box	Calabrian pine & Oak	Ash-tree			
	Cypress	Nordmann's fir & Pure Crimean Pine	Plane tree			
	Calabrian pine	Beech & Nordmann's fir & Oak	Poplar			
			Alder trees			
			Chestnut			
			Lime tree			

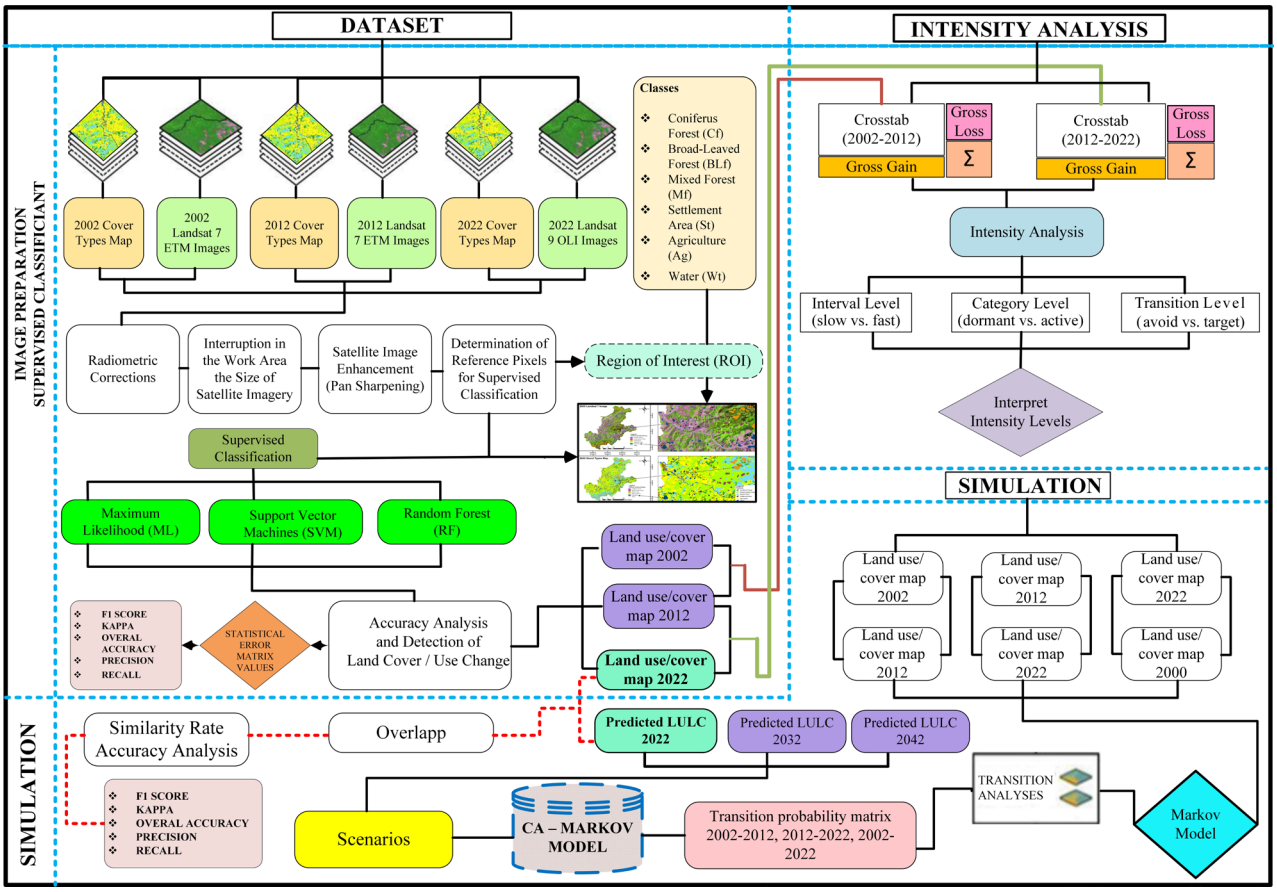

FIGURE 2: Flowchart showing the methodology of the study.

occur radiometrically in the image brightness values depending on the weather conditions at the time the image is taken, the position of the sun, the cloudiness rate, the sensor, the wavelength of the reflection, atmospheric and topographic effects. To minimise the lines in the study, the radiometric errors in the images were corrected with ENVI software so that the root mean square error (RMSE) was less than one pixel. Then, a band combination process was performed on the images of each year (2002, 2012, 2022). Bands 5, 4, and 3 were used for Landsat 7 ETM, bands 6, 5, and 4 in combination were used for Landsat 8 OLI, and the composite image was clipped to the study area. Classification success is directly proportional to the quality and clarity of the images used. For this reason, images were made ready for classification by applying image enrichment (Pan Sharpening) to increase the perceptibility, interpretability, quality, and qualification of the images.

A total of six land use classes were defined in the study from the forest area class; coniferous, broad-leaved, and mixed forest, and from the non-forest lands; settlement, agriculture, and water. The reference pixels (ROI) required for the classification process were determined according to the intensity and distribution of the classes in the field, using forest type maps for 2002, 2012, and 2022, GPS data of terrestrial measurements, and Google Earth images. Snedecor and Cochran's (1969) methods were used to determine the minimum number of sample pixels in the reference pixels taken (Equation 1). The minimum number of reference pixels for each class was set to 204 for 85% accuracy and a 5% maximum error rate.

$$N = 4pq / E \quad (1)$$

Where N is the total number of pixels to sample; p is the expected percent accuracy; q equals 100-p; and E is the maximum allowable percentage of error:

In the study, three supervised classification methods were used. The first of these was the MLC method, which is a statistical-based classification method that takes into account the mean-variance and covariance values. In MLC, probability intensity functions at the classification stage are calculated and the pixels to be classified are assigned to a higher class. The second one was the SVM method based on the structural risk minimisation principle and statistical learning theory. In SVM, the goal is to obtain optimal hyper-level classes. With the distance between the resulting hyper-level and support vectors, the most stable class function maximised is generated (Kulkarni & Lowe 2016; Günlü 2021). In the third technique, the RF method, a random subset is sampled (classes) by giving a training set, and a decision tree pattern is created for similar classes. After these repetitive patterns are terminated, the image is

classified using the decision tree pattern that provides the greatest similarity for the classes (Kulkarni and Lowe 2016).

The classification accuracy of the images classified by each method was checked with Kappa statistics and F1-Score. Kappa in statistics; overall accuracy indicates how well the obtained classification result matches the actual situation in the field, and the producer's accuracy indicates how well each class is classified with sample pixels. User's accuracy, on the other hand, shows how many of the pixels of the user's real situation in the terrain are correctly represented on the classified map. Finally, the Kappa coefficient (κ) shows the actual consistency between the reference data and the classified map (Congalton & Gren 2019; Aksoy & Kaptan 2021). In F1-Score, Precision refers to the ratio of correctly classified pixels to the sum of false and negative pixels. Recall, on the other hand, is expressed as the ratio of correctly classified pixels to all pixels. Finally, the F1-Score is an evaluation criterion expressed with the harmonic mean of Precision and Recall (Yacouby & Axman 2020).

Intensity analysis

Intensity analysis, developed by Aldwaik and Pontius (2012), calculates the transitions between categories in terms of size and intensity, at three different levels: time interval, category level, and transition level. To perform the analysis, land change matrix tables of the study periods should be created. Because in intensity analysis, the amount of variation between categories in the time intervals of the study constitutes the input data. The basic rationale for the analysis is to compare changes across the entire temporal and spatial extent with uniform intensity, which assumes that their intensities are evenly distributed (Aldwaik & Pontius Jr 2012; Anteneh et al. 2018; Kaptan 2021).

Time-interval intensity analysis compares the size and rate of change for each time interval with uniform intensity, which is calculated as the rate of change for the entire working period. If the annual change intensity (S_t) value obtained according to the calculation made according to Equation 2 for each time interval is higher than the uniform intensity (U) value calculated according to Equation 3, then the rate of change is interpreted as high for the relevant time interval, and low if it is less (Aldwaik & Pontius 2012; Kaptan 2021).

$$S_t = \frac{(\text{area of change during interval } [Y_t, Y_{t+1}]) \,/\, (\text{area of study region})}{\text{duration of interval } [Y_t, Y_{t+1}]} \times 100$$

$$\% = \frac{\{\sum_{j=1}^{J}[(\sum_{i=1}^{J} C_{tij}) - C_{tjj}]\} \,/\, [\sum_{j=1}^{J}(\sum_{i=1}^{J} C_{tij})]}{[Y_{t+1} - Y_t]} \times 100\% \quad (2)$$

$$U = \frac{(\text{area of change during all intervals})/(\text{area of study region})}{\text{duration of all intervals}} \times 100$$

$$\% = \frac{\sum_{t=1}^{T-1}\{\sum_{j=1}^{J}[(\sum_{i=1}^{J} C_{tij}) - C_{tjj}]\} \,/\, [\sum_{j=1}^{J}(\sum_{i=1}^{J} C_{tij})]}{[Y_T - Y_1]} \times 100\% \quad (3)$$

Where J = number of categories; i = index for a category at an initial time; j = index for a category at a subsequent time; T = number of time points; t = index for a time point, which ranges from 1 to $T - 1$; Y_t = year at time point t; Ct_{ij} = number of pixels that transition from category i at time Y_t to category j at time Y_{t+1}.

The category level examines how the gross gains (Equation 4) and gross losses (Equation 5) of each category at each time interval vary between categories, in terms of size and intensity (Huang et al. 2012). The analysis compares the annual gain intensity (G_{tj}) and loss intensity (L_{ti}) of each category with the annual change intensity (S_t) calculated according to Equation 2 for the relevant period. In this way, it is determined which category is active or dormant in terms of loss and gain during the time interval.

$$G_{tj} = \frac{(\text{area of gross gain of category } j \text{ during } [Y_t, Y_{t+1}]) \,/\, (\text{duration of } [Y_t, Y_{t+1}])}{\text{area of category } j \text{ at time } Y_{t+1}} \times 100$$

$$\% = \frac{[(\sum_{i=1}^{J} C_{tij}) - C_{tjj}] \,/\, (Y_{t+1} - Y_t)}{\sum_{i=1}^{J} C_{tij}} \times 100\% \quad (4)$$

$$L_{ti} = \frac{(\text{area of gross loss of category } i \text{ during } [Y_t, Y_{t+1}]) \,/\, (\text{duration of } [Y_t, Y_{t+1}])}{\text{area of ategory } i \text{ at time } Y_t} \times 100$$

$$\% = \frac{[(\sum_{j=1}^{J} C_{tij}) - C_{tii}] \,/\, (Y_{t+1} - Y_t)}{\sum_{j=1}^{J} C_{tij}} \times 100\% \quad (5)$$

The transition level examines the gross gains of each category in each time period from which categories' gross losses are derived from the transitions. The analysis for this gives the annual transition intensity (R_{tin}) observed from category i to category n during the time interval according to the size of category i in the starting year (Y_t) of the relevant time interval, according to Equation 6. The R_{tin} value is compared to the annual uniform transition intensity (W_t) calculated according to Equation 7 and based on the assumption that category n acquires evenly across the entire landscape. If $R_{tin} < W_{tn}$ is small, category i losses in time interval t mean that category n avoids targeting as gain, if $R_{tin} > W_{tn}$ is large, category n is targeted as gain (Kaptan 2021).

$$R_{tin} = \frac{(\text{area of transition from } i \text{ to } n \text{ during } [Y_t, Y_{t+1}]) \,/\, (\text{duration of } [Y_t, Y_{t+1}])}{\text{area of category } i \text{ at time } Y_t} \times 100$$

$$\% = \frac{C_{tin} \,/\, (Y_{t+1} - Y_t)}{\sum_{j=1}^{J} C_{tij}} \times 100\% \quad (6)$$

$$W_{tn} = \frac{(\text{area of gross gain of category } n \text{ during } [Y_t, Y_{t+1}]) \,/\, (\text{duration of } [Y_t, Y_{t+1}])}{\text{area that is not category } n \text{ at time } Y_t} \times 100$$

$$\% = \frac{[(\sum_{i=1}^{J} C_{tin}) - C_{tnn}] \,/\, (Y_{t+1} - Y_t)}{\sum_{j=1}^{J}[(\sum_{i=1}^{J} C_{tij}) - C_{tnj}]} \times 100\% \quad (7)$$

Scenario modelling (Cellular Automaton-Markov model) and validation

A Markov chain is a model that makes predictions using the probability of transition from the current state to the next state (Guan et al. 2008). This model includes the logic of simulating the next period depending on the state of the previous period, using the inter-period change-

transition probability matrix (Wang & Murayama 2017; Aksoy & Kaptan 2022). In this study, a land use model at a given time is equivalent to a state of the Markov process, and the area varying between land use models is the ratio of state transition probability. Equation 8 shows the Markov estimate (Huang et al. 2020).

$$Z_{(l+1)} = Z_l \times Q \quad (8)$$

Where $Z_{(l+1),}$ represents the LULC state at time l+1, whereas Z_l represents the LULC state. Time Q represents the probability matrix of transition from time l to time slot l+1.

$$Z = [Z_1 Z_2 Z_3 Z_4 Z_5 Z_6] \quad (9)$$

Z_i (i=1, 2, ……, 6) indicates coniferous forest, leafy forest, mixed forest, residential area, agriculture, and water bodies usage areas, respectively (Equation 9), Q can be defined as a [n, n] matrix below (Equation 10). Here, n refers to the total number of land use patterns, Q_{ij} = probability of transition from i to j in the land use pattern, while it also states that the sum of each row of the matrix should be equal to 1.

$$Q = \begin{bmatrix} Q_{11} & Q_{12} & \cdots & Q_{1n} \\ Q_{21} & Q_{22} & \cdots & Q_{2n} \\ \vdots & \vdots & \vdots & \vdots \\ Q_{n1} & Q_{n2} & \cdots & Q_{nn} \end{bmatrix}, \sum_{(j=1)}^{n} Q_{ij} = 1, 1 \le i,j \le n, n = 6 \quad (10)$$

A standard *CA* model is divided into four features: discrete cellular (D), finite state (S), neighbour (L), and rules (R). According to a particular transformation function, the next state cell is determined by the current state and its neighbour. The four directions can be defined as:

$$CA = (D, S, L, R) \quad (11)$$

Where CA, D, S, L, and R parameters are defined as the Cellular Automata system, size of any positive integer, discrete state, neighbourhood, and rules, respectively (Equation 11). In particular, L is as follows (Equation 12);

$$L = (S_1, S_2, S_3, \cdots, S_n), S_n \in S$$

Here n is the number of neighbours (Huang et al. 2020).

In the current study, LULC scenarios (2022, 2032, 2042) were carried out using Cellular Automata (CA) and Markov chain analysis modelling. The period used in the Cellular Automaton/Markov chain change analysis was then used as the starting point for the LULC change simulation (the year 2022). Cellular Automaton iteration count and a standard 5 x 5 contiguous filter were applied based on the number of times it took for forward projection specified in Markov chain analysis.

Results

Classification and accuracy assessment

The LULC maps of the study area were classified as supervised by three different classification methods by reference to 2002, 2012, and 2022 forest type maps. Images of the most successful classification method for each year were used for analysis. The accuracy values and error matrix of three different classification techniques for each period are shown in Tables 3A, B & C.

The most successful classification for 2002 was obtained by the Maximum Likelihood Classification (MLC) method (Kappa =0.88, F1-Score = 0.86), Table 3A. Overall Accuracy was found as 0.94 for the 2002 LULC map. The results of the three classification methods show that the classification is successful and that the ability to represent the field of study is high. In the analysis, the LULC map obtained with the 2002 MLC method was used.

The highest success in the classification for 2012 was obtained in the MLC method as in 2002 (Kappa = 0.78, F1-Score = 0.83), Table 3B. Overall Accuracy was found as 0.83. The highest F1-Score values (≥80%), respectively; Water, Coniferous Forest, Broad-Leaved Forest, and Agriculture classes. The precision value was over 80% in all classes except for Mixed Forest and Agriculture classes (Table 3B). Finally, the classification accuracy values and error matrix for 2022 are shown in Table 3C. As in the other two periods, the most successful LULC of 2022 was obtained from the MLC method (Kappa = 0.81, F1-Score = 0.86). Overall Accuracy was found as 0.86. F1-Score values also show that high (≥80%) classification achievements have been achieved for all classes.

The most successful classification of 2002, 2012, and 2022 was obtained in the MLC method for each year. In all periods, after MLC, the most successful method was found to be SVM and RF, respectively. A Kappa coefficient of ≤ 0 means there is no fit, 0–0.2 a slight fit, 0.2–0.41 an average fit, 0.41–0.60 a moderate to intermediate level of fit, 0.60–0.80 a significant fit, and 0.81–1.0 a perfect fit. (Patekar et al. 2013). When the methods of all classifications are evaluated, the Kappa and F1-Score being above 70% indicate that all the methods used in the study can be used in the classification at moderate and significant levels. The LULC maps produced by the MLC method for each year are shown in Figure 3. In the classification, a total of six land use classes were determined as Coniferous Forest (CF), Mixed Forest (MF), Broad-Leaved Forest (BLF), Settlement (St) Agriculture (Ag), Water (Wt). It was determined that proportionally large changes occurred in water and settlement classes. The part where the row and column of the same class overlap, which is expressed in bold in the error matrices for all periods, represents the number of correctly classified pixels of the relevant class. In Figure 3, it is seen that the ratio of area to the number of representative pixels selected (Table 4) is directly proportional.

TABLE 3A: Classification maps accuracy and error matrix values of 2002.

Method	Class[1]	CF	MF	BLF	St	Ag	Wt	Total	Prod Acc.	User Acc.	Precision (%)	Recall (%)	F1 Score (%)	Overall F1 Score (%)	Overall Acc. (%)	Kappa (%)
	CF	***13774***	2017	204	530	3061	850	20436	86.73	67.4	0.867	0.674	0.759			
	MF	481	***59091***	14065	57	339	0	74033	90.65	79.82	0.907	0.798	0.849			
	BLF	153	2853	***177975***	241	3395	0	184617	87.75	96.4	0.878	0.964	0.919			
MLC	**St**	32	56	3707	***1207839***	4672	714	1217020	96.35	99.25	0.963	0.992	0.978	0.86	0.94	0.88
	Ag	718	1166	6832	38584	***146216***	1828	195344	90.6	74.85	0.906	0.749	0.820			
	Wt	724	2	28	6390	3705	***41221***	52070	92.4	79.16	0.924	0.792	0.853			
	Total	15882	65185	202811	1253641	161388	44613	***1743520***								
	CF	***45172***	1734	219	262	655	1754	49796	48.6	90.71	0.486	0.907	0.633			
	MF	1373	***55201***	6069	88	1537	4	64272	90.36	85.89	0.904	0.859	0.881			
	BLF	17	1893	***86362***	325	1760	21	90378	90.36	95.56	0.904	0.956	0.929			
SVM	**St**	245	146	903	***15808***	9579	1633	28314	76.44	55.83	0.764	0.558	0.645	0.79	0.76	0.71
	Ag	595	380	1653	3474	***61100***	2373	69575	78	87.82	0.780	0.878	0.826			
	Wt	373	1	155	461	3052	***30147***	34189	80	88.18	0.800	0.882	0.839			
	Total	92947	61089	95580	20680	78338	37686	***386320***								
	CF	***45302***	2097	110	240	458	3242	51449	48.67	88.05	0.487	0.881	0.627			
	MF	1061	***54379***	5501	111	1317	0	62369	88.49	87.19	0.885	0.872	0.878			
	BLF	20	2422	***86859***	234	2328	11	91874	90.98	94.54	0.910	0.945	0.927			
RF	**St**	184	102	805	***16684***	15001	2485	35261	80.76	47.32	0.808	0.473	0.597	0.77	0.74	0.69
	Ag	617	350	1960	2780	***55536***	2314	63557	71.07	87.38	0.711	0.874	0.784			
	Wt	591	5	126	369	3043	***27880***	32014	71.17	87.09	0.712	0.871	0.783			
	Total	93077	61452	95471	20658	78141	39174	***387973***								

[1] CF = Coniferous forest; MF = Mixed forest; BLF = Broad-leaved forest; Ag = Agriculture; Wt - water. See Table 2 for details of each class

TABLE 3B: Classification maps accuracy and error matrix values of 2012.

Method	Class[1]								Prod Acc.	User Acc.	Precision (%)	Recall (%)	F1 Score (%)	Overall F1 Score (%)	Overall Acc. (%)	Kappa (%)
Method	**Class[1]**	**CF**	**MF**	**BLF**	**St**	**Ag**	**Wt**	**Total**								
	CF	***42952***	6856	142	280	1174	9	51413	93.36	83.54	0.93	0.84	0.88			
	MF	911	***34266***	2514	522	3075	25	41313	63.35	82.94	0.63	0.83	0.72			
	BLF	276	11161	***81724***	171	7930	0	101262	94.24	80.71	0.94	0.81	0.87			
MLC	**St**	901	858	169	***20140***	6806	336	29210	79.95	68.95	0.80	0.69	0.74	0.83	0.83	0.78
	Ag	952	953	2152	4056	***65795***	495	74403	77.32	88.43	0.77	0.88	0.83			
	Wt	16	0	15	22	317	***9603***	9973	91.74	96.29	0.92	0.96	0.94			
	Total	46008	54094	86716	25191	85097	10468	***307574***								
	CF	***42725***	2403	62	321	773	31	46315	48.15	92.25	0.48	0.92	0.63			
	MF	2270	***48626***	6340	546	977	1	58760	86.07	82.75	0.86	0.83	0.84			
	BLF	67	2314	***77787***	81	2366	4	82619	89.64	94.15	0.90	0.94	0.92			
SVM	**St**	197	207	232	***18642***	5102	129	24509	73.07	76.06	0.73	0.76	0.75	0.82	0.77	0.72
	Ag	722	534	2295	4271	***75416***	319	83557	87.84	90.26	0.88	0.90	0.89			
	Wt	27	9	0	1329	451	***9983***	11799	95.09	84.61	0.95	0.85	0.90			
	Total	88733	56496	86778	25511	85858	10498	***353874***								
	CF	***43186***	2373	45	222	606	35	46467	48.42	92.94	0.48	0.93	0.64			
	MF	1372	***48728***	5770	373	662	3	56908	86.30	85.63	0.86	0.86	0.86			
	BLF	91	2238	***78589***	76	3307	0	84301	90.58	93.22	0.91	0.93	0.92			
RF	**St**	173	266	239	***21684***	9961	204	32527	85.33	66.66	0.85	0.67	0.75	0.82	0.77	0.72
	Ag	1179	459	2066	2649	***69842***	373	76568	81.50	91.22	0.82	0.91	0.86			
	Wt	7	29	7	186	707	***9852***	10788	93.81	91.32	0.94	0.91	0.93			
	Total	89194	56466	86761	25412	85691	10502	***354026***								

[1] CF = Coniferous forest; MF = Mixed forest; BLF = Broad-leaved forest; Ag = Agriculture; Wt - water. See Table 2 for details of each class

TABLE 3C: Classification maps accuracy and error matrix values of 2022.

Method	Class[1]								Prod Acc.	User Acc.	Precision (%)	Recall (%)	F1 Score (%)	Overall F1 Score (%)	Overall Acc. (%)	Kappa (%)
Method	**Class[1]**	**CF**	**MF**	**BLF**	**St**	**Ag**	**Wt**	**Total**								
	CF	***22231***	1918	52	13	413	11	24638	93.67	90.23	0.94	0.90	0.92			
	MF	933	***24907***	6159	6	901	0	32906	86.53	75.69	0.87	0.76	0.81			
	BLF	76	1670	***57437***	58	9105	0	68346	86.87	84.04	0.87	0.84	0.85			
MLC	**St**	93	8	206	***19516***	5804	506	26133	85.82	74.68	0.86	0.75	0.80	0.86	0.86	0.81
	Ag	171	280	2256	2952	***60930***	265	66854	78.94	91.14	0.79	0.91	0.85			
	Wt	229	1	11	195	34	***10659***	11129	93.16	95.78	0.93	0.96	0.94			
	Total	23733	28784	66121	22740	77187	11441	**230006**								
	CF	***15067***	1652	66	16	287	42	17130	48.08	87.96	0.48	0.88	0.62			
	MF	1040	***17903***	4924	69	1480	9	25425	77.43	70.41	0.77	0.70	0.74			
	BLF	10	1619	***51438***	41	3767	0	56875	86.41	90.44	0.86	0.90	0.88			
SVM	**St**	3	6	82	***11908***	5581	126	17706	84.95	67.25	0.85	0.67	0.75	0.81	0.79	0.73
	Ag	110	283	2944	1792	***59142***	93	64364	83.68	91.89	0.84	0.92	0.88			
	Wt	38	6	11	175	130	***10197***	10557	97.03	96.59	0.97	0.97	0.97			
	Total	31335	23121	59531	14017	70674	**10509**	**209187**								
	CF	***22371***	1758	60	243	305	44	24781	48.52	90.27	0.49	0.90	0.63			
	MF	1216	***24957***	5394	37	1669	5	33278	81.71	75.00	0.82	0.75	0.78			
	BLF	16	1765	***56298***	65	4706	0	62850	85.07	89.58	0.85	0.90	0.87			
RF	**St**	7	4	144	***20145***	10965	333	31598	87.90	63.75	0.88	0.64	0.74	0.80	0.76	0.71
	Ag	105	296	4215	1728	***59434***	199	65977	76.71	90.08	0.77	0.90	0.83			
	Wt	18	4	10	457	96	***10859***	11444	94.56	94.89	0.95	0.95	0.95			
	Total	46104	30542	66181	22918	77480	11484	**254709**								

[1] CF = Coniferous forest; MF = Mixed forest; BLF = Broad-leaved forest; Ag = Agriculture; Wt - water. See Table 2 for details of each class

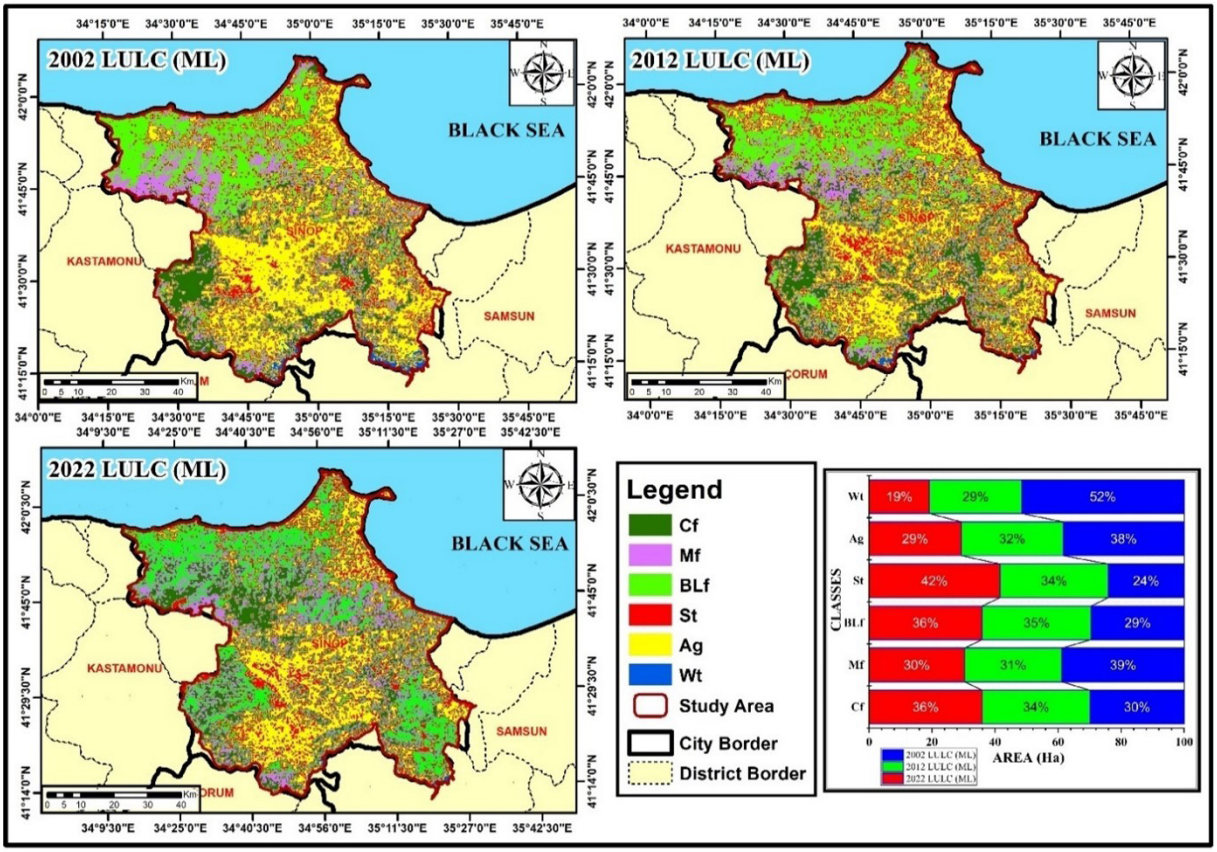

FIGURE 3: LULC maps of classified images of the study area for three years (2002, 2012, and 2022).

Land change for the years 2002, 2012 and 2022

The changes at the end of the years of the LULC categories are shown in real and percentage terms in Table 5 and visually in Figure 3. The results show that only mixed forest decreased by 22% in the forest area class in 2002-2022, while coniferous- and broad-leaved forests increased by 20% and 22% respectively. Only one category of non-forest area was found to have increased. This category is Settlement, which has a remarkably high value of 72%, whereas agriculture and water have continued to decrease over the years.

Although settlements have increased and mixed-forest areas have decreased, increases in coniferous and broad-leaved forest have contributed to an increase of 37,823.38 ha (12.91%) in forest areas from 2002 to 2022. It is precisely at this point that looking at the results of the intensity analysis, which is the main subject of the study, and making evaluations will contribute to more consistent results and interpretations.

Intensity analysis

Interval level

According to the land use change matrix for the 2002-2012 and 2012-2022 time periods, the total amount of land-use change in each period, annual change intensity, and intensity of change are shown in Figure 4.

The bars at the top of the graph show the intensity of the observed changes, and each bar at the bottom shows the percentage of change level experienced in the time intervals. The fact that the 2002-2012 period bar (annual change rate 4.15%) at the top is above the uniform line (3.92%) indicates that the rate of land use change is fast in this period, while the 2012-2022 period bar (annual rate of change 3.69%) is below the uniform line, shows that the rate of change is slow in this period. If both bars were together above the uniform line, it would mean that the annual changes in categories were constant over the entire temporal scope.

Category level

According to the basic logic of intensity analysis, comparisons are made according to the uniform intensity, which expresses the assumption that the intensities of the changes experienced throughout the entire temporal and spatial scope are equally distributed. If the bar of a category goes above the uniform line, it means that the gain or loss intensity for the relevant category is more intense (active) compared to the general working area, if it ends before it reaches the uniform line, it is dormant, that is, it is less dense than the overall work area.

The results of the category level of the intensity analysis showing the annual area changes and the change intensities of each category in terms of gross loss and gross gain in each period are given in Figure 5. The top side of the graph shows the intensity of change in gains and losses for each category, and the bottom side shows only the variation of annual observed gains and losses in the area.

TABLE 4: LULC transition probabilities matrix for the 2002-2022 periods of the study area.

Transitional probabilities matrices for LULC (ha) of the Sinop Forest for the period 2002 - 2022						
Class[1]	**2002- 2012**					
	CF	**MF**	**BLF**	**St**	**Ag**	**Wt**
CF	**0.7187**	0.0297	0.0501	0.0445	0.1439	0.013
MF	0.1658	**0.3125**	0.4851	0.0126	0.0229	0.0011
BLF	0.0495	0.1171	**0.685**	0.0153	0.1324	0.0007
St	0.1541	0.0181	0.0212	**0.2908**	0.5015	0.0143
Ag	0.0834	0.0423	0.1397	0.1268	**0.5983**	0.0094
Wt	0.3152	0.0209	0.0111	0.1157	0.2721	**0.265**
Class[1]	**2012- 2022**					
	CF	**MF**	**BLF**	**St**	**Ag**	**Wt**
CF	**0.6007**	0.0851	0.0827	0.0745	0.1506	0.0064
MF	0.4353	**0.2319**	0.1511	0.049	0.131	0.0018
BLF	0.1582	0.1549	**0.5601**	0.0121	0.1145	0.0001
St	0.0564	0.0081	0.0902	**0.4008**	0.4392	0.0054
Ag	0.0327	0.0107	0.282	0.1188	**0.5523**	0.0034
Wt	0.1377	0.0068	0.0181	0.1332	0.2642	**0.44**
Class[1]	**2002- 2022**					
	CF	**MF**	**BLF**	**St**	**Ag**	**Wt**
CF	**0.5533**	0.0572	0.1178	0.0881	0.175	0.0086
MF	0.4165	**0.2802**	0.2387	0.0345	0.0293	0.0009
BLF	0.1863	0.1416	**0.5577**	0.0199	0.0943	0.0001
St	0.1088	0.0058	0.181	**0.2738**	0.4231	0.0074
Ag	0.0701	0.0239	0.2513	0.1348	**0.5148**	0.0051
Wt	0.1492	0	0.0807	0.1651	0.4023	**0.2028**

[1] CF = Coniferous forest; MF = Mixed forest; BLF = Broad-leaved forest; Ag = Agriculture; Wt - water. See Table 2 for details of each class

The gains of the broad-leaved forest and coniferous forest categories, which are in the forest area class, are higher than their losses in the first-time interval, and the losses of the mixed forest category are higher than their gains. In the second time interval, this situation was exactly the opposite, while the gain of the mixed forest category was higher than the loss, the losses observed in the broad-leaved forest and coniferous forest categories were higher than the gain. In the non-forest area class; While the losses of agriculture and water categories were higher than the gains in the 2002-2012 time period, this situation was the opposite in the 2012-2022 time period. On the other hand, the gain of the settlement category is higher than the loss in both time intervals.

To better understand the transitions between categories, it is necessary to look at the annual intensity changes of each category. In the first time interval, broad-leaved forest is active only in terms of gain, while mixed forest is active in terms of both gain and loss. The mixed forest category was the category that experienced the most intense loss whereas coniferous forest remained the same. In the second time interval, the broad-leaved

TABLE 5: Changes in area of land use/land cover for the period 2002-2022 (ha, %).

Class[1]	**2002 (ha)**	**%**	**2012 (ha)**	**%**	**2022 (ha)**	**%**	**2002-2022 (+/-)**	**+/- %**
CF	104,878.30	19	120,027.45	22	126,368.71	23	21,490.41	20
MF	56,338.43	10	44,964.82	8	44,093	8	-12,245.43	-22
BLF	131,755.18	24	154,909.25	28	160,333.58	29	28,578.40	22
St	30,853.51	6	43,966.08	8	53,215.24	10	22,361.73	72
Ag	219,121.32	39	184,815.47	33	167,276.17	30	-51,845.15	-24
Wt	13,293.79	2	7,557.46	1	4,953.84	1	-8,339.95	-63
Total	556,240.53	100	556,240.53	100	556,240.53	100		

[1] CF = Coniferous forest; MF = Mixed forest; BLF = Broad-leaved forest; Ag = Agriculture; Wt - water. See Table 2 for details of each class

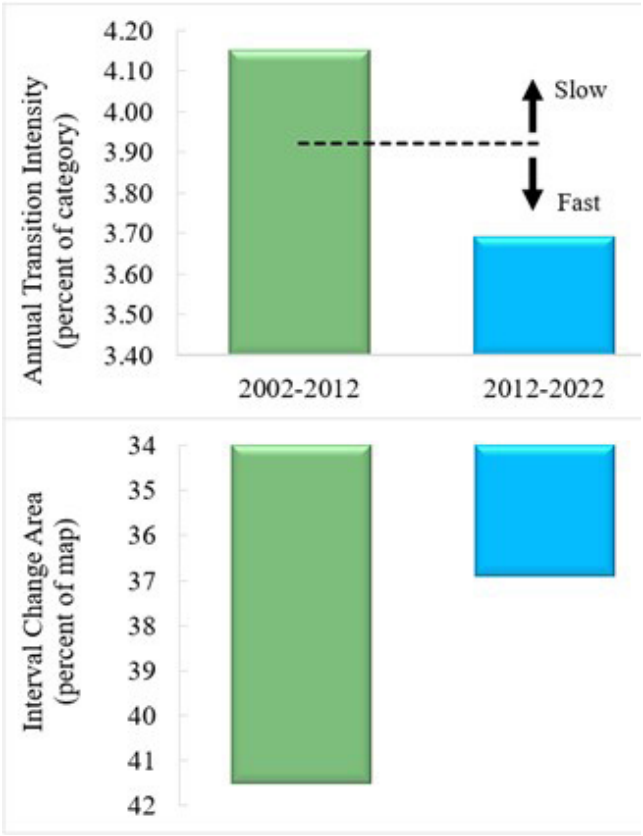

FIGURE 4: Interval-level intensity analysis for the time periods 2002-2012 and 2012-2022.

forest category switched to the active loser status, while the mixed forest category remained active in terms of both gain and loss and became a winner in the second period. The coniferous forest category, which is dormant in the first time interval, is active in terms of loss in the second time interval. In the non-forest area class, the agriculture category is dormant in terms of loss and gain in both time periods. The settlement category is active in both time slots in terms of losses and gains, and is also in a heavy winner state. water category, on the other hand, was an active loser in the first time slot, and became an active winner in the second time slot.

Transition level

The results of the transition level analysis, which show which categories' gains and losses of each category mainly target the losses, are given in Figure 6 for the categories included in the forest area class and Figure 7 for those in the non-forest area class. The top of each graph shows the intensity of annual passes, and the bottom shows the size of annual passes. According to the analysis results, While the broad-leaved forest category heavily targeted the losses of the mixed forest category as gains in the 2002-2012 time period, it targeted the losses of both the mixed forest and agriculture categories in the 2012-2022 time period. While the gain of the coniferous forest category targeted the losses of both mixed forest and water categories in the first time interval, it targeted the losses of the mixed forest category most intensely in the second time interval. The gain of mixed forest targeted

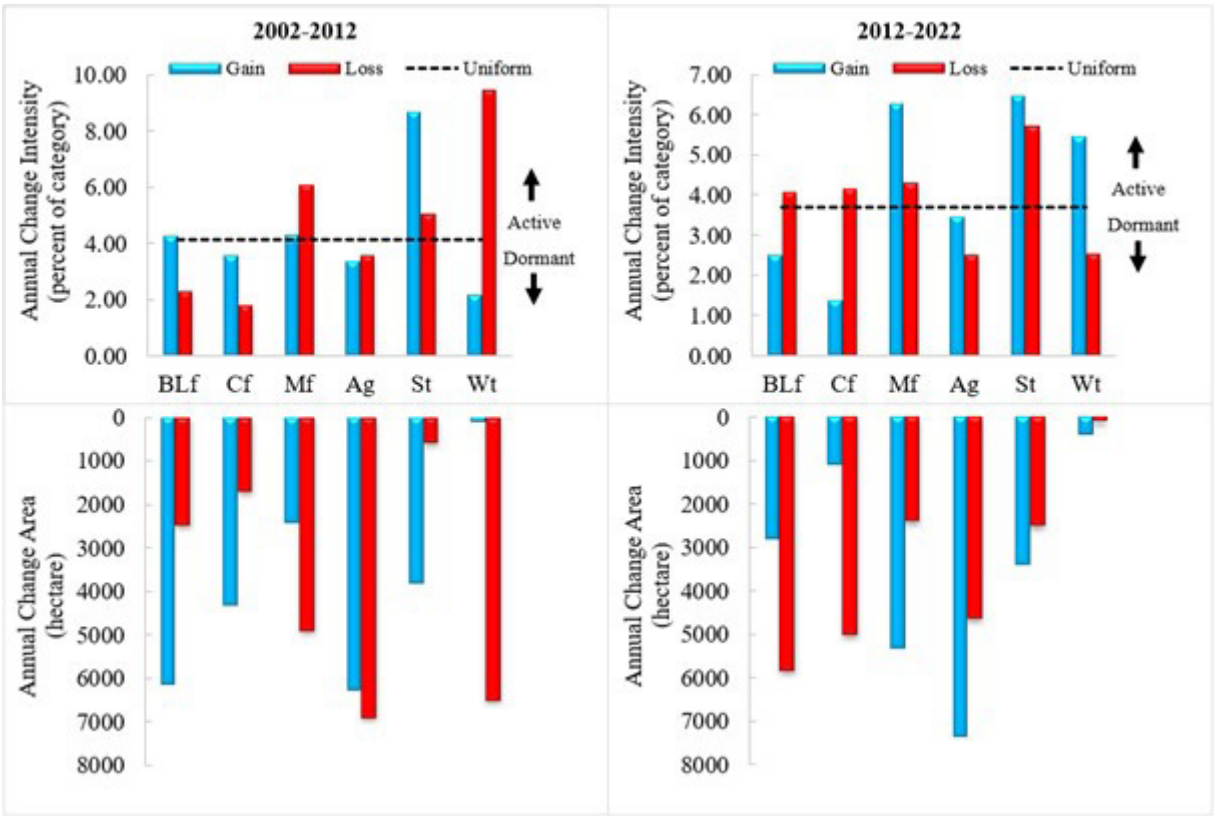

FIGURE 5: Category level showing active losing and gaining categories for time intervals.

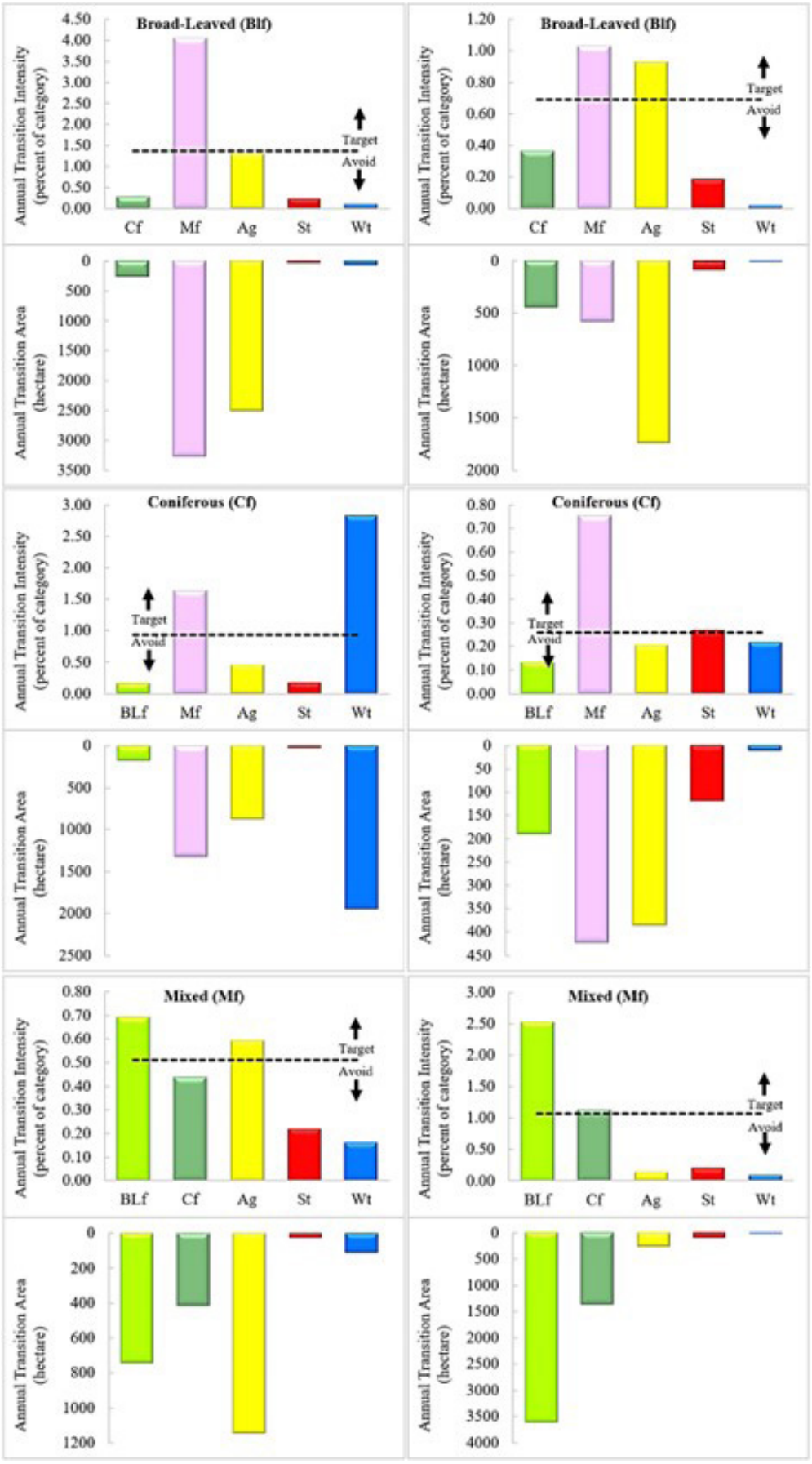

FIGURE 6: Transition intensity analysis for the gains of categories within forest class during the two-time intervals (a. 2002-2012; b. 2012-2022).

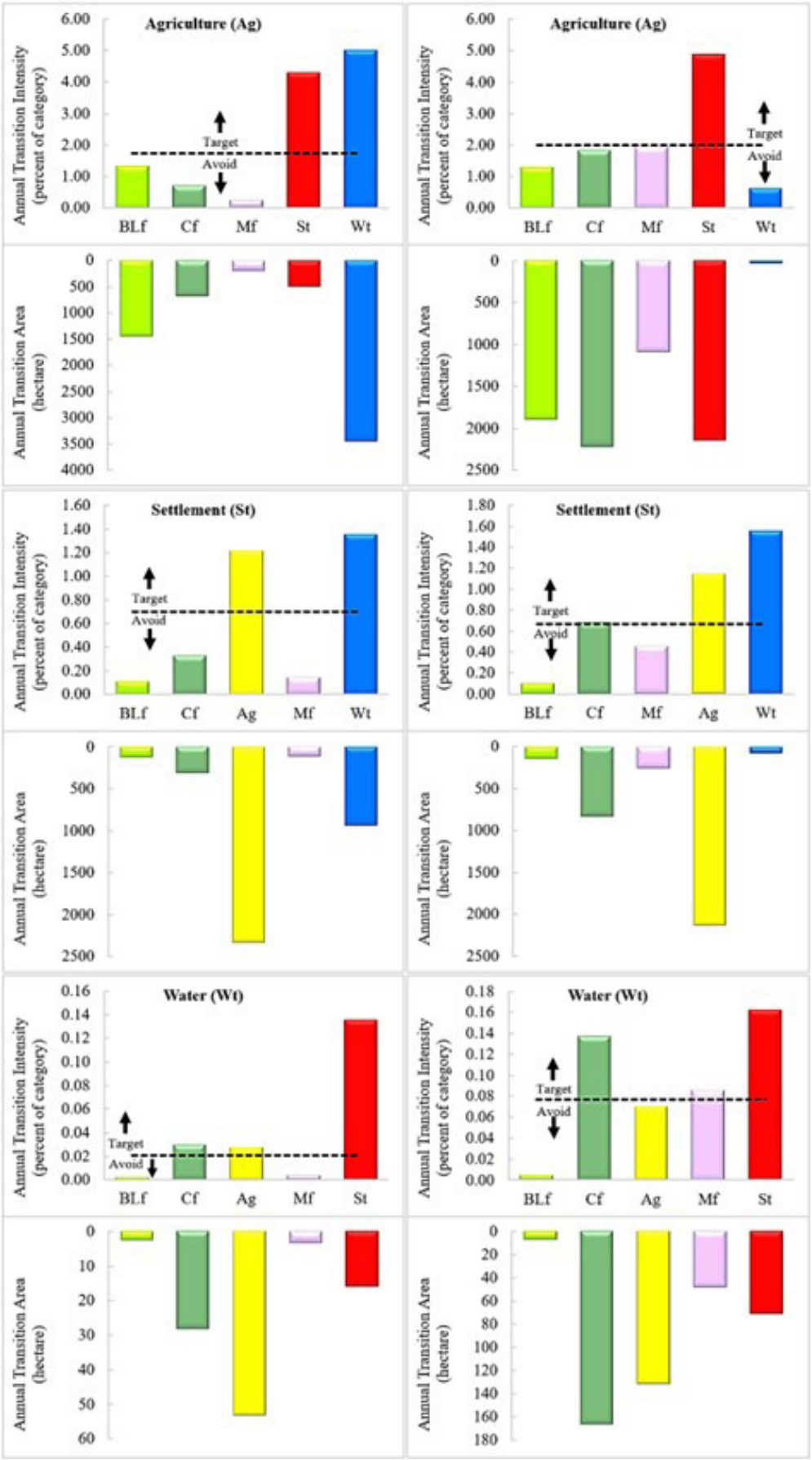

FIGURE 7: Transition intensity analysis for the gains of categories within the non-forest class during the two-time intervals (a. 2002-2012; b. 2012-2022).

the losses of the broad-leaved forest and agriculture categories in the first timeframe, and the losses of the broad-leaved forest and partially coniferous forest categories in the second timeframe as gains.

According to Figure 8, the results of the transition-level analysis, show which gains in categories corresponded with losses of each category in the non-forest area class. While agriculture targeted water and settlement losses as gains in the first time slot, it targeted only settlement losses in the second time slot. Settlement both in the first and second time slots agriculture and water aimed to gain their losses. The water category, on the other hand, targeted coniferous forest and settlement losses in both timeframes, while most intensely targeted settlement losses as gains. Especially in the second time interval, it is seen that the water category targets coniferous forest losses more intensely compared to the first time interval.

Markov validation and scenario modelling

In the study, the LULC map of 2022 was tried to be estimated by calculating the transition probability matrix from the LULC maps obtained with the 2002-2012 classification. The LULC simulation map of 2032 was generated using LULC transition probabilities matrix values for the period 2012-2022. 2042 LULC simulation map was produced using the LULC transition probabilities matrix values for the period 2002-2022 (Table 4, Figure 9).

In the transition probabilities matrix (Table 4) the rows show the land use class values for the previous period and the columns show the land use class values for the next period. Diagonal values show the probability of each class remaining unchanged. In other words, the diagonal part shows the resistance of the relevant class to the transition. From these data, the most resistant classes to transition in all periods are coniferous forest and broad-leaved forest. It is seen that the classes most inclined to the transition without resistance are settlement and water. In the Intensity analysis, it was determined that the losses and gains were realised between coniferous forest, broad-leaved forest, settlement, and water with the highest ratio.

Accuracy assessment of the CA-Markov model

The Markov model was checked with the estimated 2022 LULC map, Kappa, and F1-Score values with the ROIs used in the 2022 LULC classification (Table 6). Along with these, model performance was also checked with Taylor diagram and dendrogram graphs (Figure 8). The estimated 2022 LULC Kappa and F1-Score values were calculated as 0.86 and 0.88, respectively. All performance criteria show that the model is highly predictive, reliable, and usable (Overall accuracy, 88.87%).

When the Taylor diagram was examined, it was determined that it was a model with a low standard deviation in the range of 0.01 to 0.02 and a high predictive

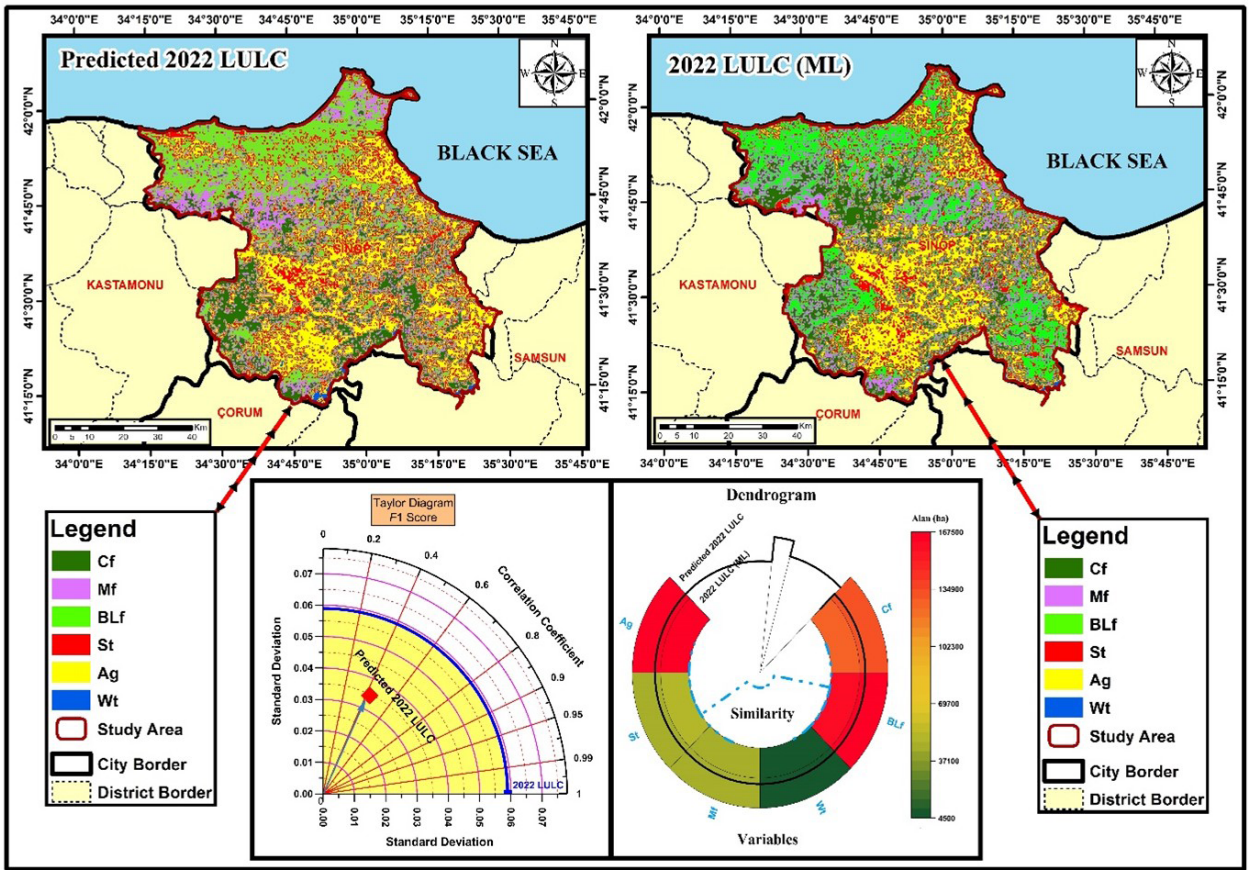

FIGURE 8: 2022 LULC maps, Taylor Diagram and Dendrogram.

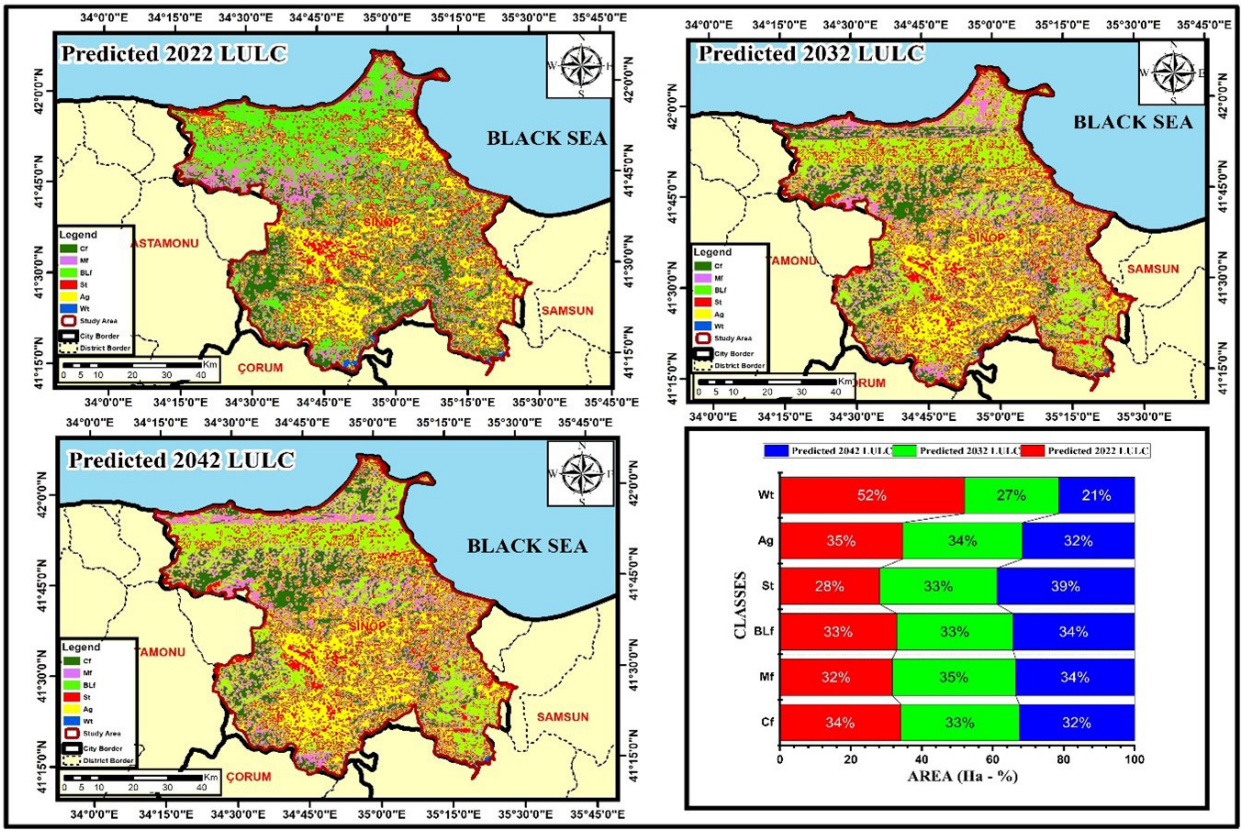

FIGURE 9: LULC maps for the years 2022, 2032, and 2042 were produced with the Cellular Automata-Markov model.

ability with a correlation greater than 0.8. Again, in the dendrogram, the fact that each land use class has a high level of overlap in the area confirms the success of the model.

Predicted 2022, 2032, and 2042 LULC

2022 LULC maps were estimated using 2002-2012 transition probabilities, 2032 LULC using 2012-2022 transition probabilities, and finally 2042 LULC map 2002-2022 transition probabilities. Predicted LULC maps were divided into 6 classes, namely Coniferous Forest, Mixed Forest, Broad-Leaved Forest, Settlement Area, Agriculture, and Water, and the area amounts (ha) of each class were determined (Table 7). In all years, more than 50% of the entire area is made up of forest area, while the largest distribution area after forest belongs to the agricultural area. The Water class is the class with the lowest area in each period.

In the 20 years (2022-2042), in the forest category: the area of coniferous forest decreased by 1.15% (6,417.9 ha) whereas broad-leaved, and mixed forest area increased by 1.20% (6,701.91 ha) and 0.50% (2,513.65 ha), respectively. Coniferous forest constituted 24.7% of the overall area in 2022 but it is estimated that it will decrease by 0.51% to 23.56% by 2032, and decrease to 22.92% by 2042, with a decrease of 0.64% compared to the previous period. Broad-leaved forest represented 29.23% of the study area in 2022 and it has been estimated that it will represent 29.06% by 2032, and 30.44% by 2042, with an increase of 1.38%. The mixed forest area was projected to represent 7.79% in 2022, increasing to 8.56% in 2032, and 18.24% in 2042.

For the non-forest area, a decrease of 2.66% and 0.71% was experienced in agriculture and water classes, respectively, while an increase of 2.86% was expected in the settlement class in the 20 years between 2022 and 2042. The reduction of 14,787.25 ha in agriculture is estimated to be shared among all other classes, and the majority of this share will be shared between classes within the forest area. It is estimated that broad-leaved forest, mixed forest, and coniferous forest will receive the most shares in this share, respectively. The forecasts for 2022, 2032, and 2042 were realised with the Markov model using the matrix of transition probabilities between classes in previous periods (Figure 8). For 2022, the broad-leaved forest and agriculture classes are seen as the most resilient with close similarity. For 2032, when the transition probability matrix is analysed, mixed forest and agriculture classes are predicted to be resistant to change with high correlation. Finally, for the year 2042, agriculture (0.79) is predicted to be the most resilient class, followed by mixed forest and broad-leaved forest classes with similar correlation (Figure 10, Table 4).

Discussion

LULC changes constitute fundamental causes of numerous economic, ecological, and sociocultural issues. Particularly, alterations in land cover attributed to anthropogenic influences that can lead to deforestation

TABLE 6: 2022 simulated LULC map accuracy and error matrix values.[1]

2022 LUM Confusion matrix table and performance criteria (predicted)															
Class[1]	**CF**	**MF**	**BLF**	**St**	**Ag**	**Wt**	**Total**	**Prod Acc.**	**User Acc.**	**Precision (%)**	**Recall (%)**	**F1 Score (%)**	**Overall F1 Score (%)**	**Overall Acc. (%)**	**Kappa (%)**
CF	***23587***	1487	89	58	349	82	25652	94.11	91.95	0.94	0.92	0.93			
MF	874	***24689***	3534	85	1012	25	30219	87.55	81.70	0.88	0.82	0.85			
BLF	105	1487	***65487***	148	5368	265	72860	91.95	89.88	0.92	0.90	0.91			
St	125	104	185	***19854***	2589	1025	23882	87.16	83.13	0.87	0.83	0.85	0.88	88.87	0.86
Ag	247	368	1895	2489	***61854***	359	67212	85.88	92.03	0.86	0.92	0.89			
Wt	125	65	34	145	854	***8958***	10181	83.61	87.99	0.84	0.88	0.86			
Total	25063	28200	71224	22779	72026	10714	***230006***								

[1] CF = Coniferous forest; MF = Mixed forest; BLF = Broad-leaved forest; Ag = Agriculture; Wt - water. See Table 2 for details of each class

TABLE 7: 2022, 2032, and 2042 LULC areas value (ha).

Predicted Land Use Classes								
Date	**Area**	**Coniferous Forest**	**Mixed Forest**	**Broad-Leaved Forest**	**Total Forest**	**Settlement Area**	**Agriculture**	**Water**
2022	**ha**	133909.14	43342.45	162609.03	339860.62	42630.95	167066.11	6682.32
	%	24.07	7.79	29.23	61.10	7.66	30.03	1.20
2032	**ha**	131071.09	47606.15	161648.32	340325.56	50009.58	162482.06	3422.79
	%	23.56	8.56	29.06	61.18	8.99	29.21	0.62
2042	**ha**	127491.95	45856.10	169310.94	342658.99	58559.96	152278.86	2742.19
	%	22.92	8.24	30.44	61.60	10.53	27.38	0.49

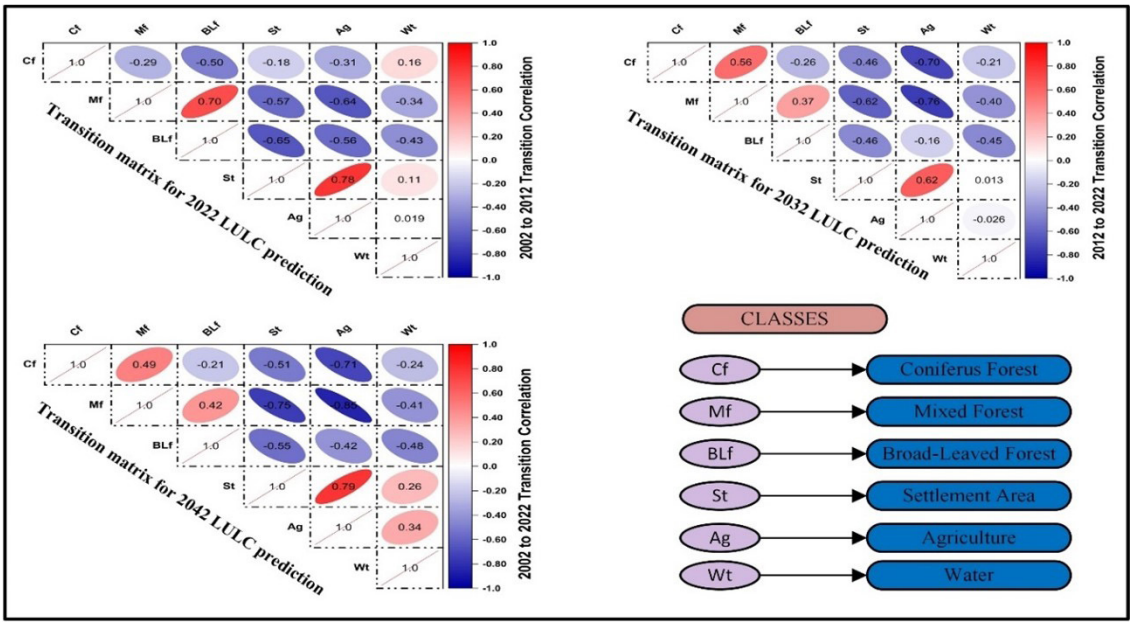

FIGURE 10: Correlation matrix of classes for periods.

serve as a primary factor for a multitude of adverse effects not only at the local but also at the global scale. Accurately mapping current and past land uses is crucial for providing reliable geographic information to model land changes, offering dependable inputs for various environmental models, and developing precise decision support systems for multidisciplinary applications. In this study, changes in six land use classes grouped under two categories, namely forest (Coniferous, Mixed, and Broad-leaved) and non-forest (Settlement, Agriculture, and Water), have been examined. Additionally, the future states of these land use classes have been predicted. Class settlement has increased by 72% during the 20 years from 2002 to 2022.

The study findings indicate that during the 20 years from 2002 to 2022, forest areas increased by 37,823.38 hectares, while non-forest areas decreased, excluding Class St. However, it would be more appropriate to focus on the intensity analysis results of the study and which land use class changes target the losses and gains of which land use class.

According to the interval-level results obtained from the intensity analysis of the study, it has been revealed that the rate of land change was faster during the period from 2002 to 2012 compared to the period from 2012 to 2022. According to the category-level results of the analysis, broad-leaved forest is in an active gaining position in the first-time interval, whereas it is in an active losing position in the second time interval. Although mixed forest was intensely active in terms of losses during the first period, it is intensely active in terms of gains during the second period. When our study results for the forested area are compared with the LULC studies of Moniruzzaman et al. (2020), Xie et al. (2021), Daba et al. (2022), it is seen that there is no similarity. In the relevant studies, contrary to our results, they identified a decrease in forested areas. It is believed that the main reason for this discrepancy stems from ecological, economic, demographic, and social structures, as well as local and regional variations. Because, the mentioned studies were conducted in areas characterised by dense and rapidly growing populations, along with industrialisation.

The regions where these studies were conducted differ from our study area in terms of population needs and requirements. In a region where industrialisation is advanced in our country, LULC was studied by Kadioğulları et al. (2014), and the results indicated a decrease in forested areas. These differences in results suggest that LULC is influenced by many factors. Yılmaz et al. (2019) and Xie et al. (2021) have argued that LULC changes are influenced by the expansion of urban and agricultural areas, deforestation, destruction of wetlands, acceleration of urbanisation, and meteorological conditions. Indeed, this statement supports our understanding of the influence of various factors on LULC. Similar to the results of our study, Aksoy and Kaptan (2021) have found in their study conducted in the northern region of Turkey that forest areas increased by 15.4% while agricultural areas decreased by 32.3% from 2000 to 2020. It can be said that several factors have contributed to the increase in forest areas in the study area. One of these factors can be attributed to the intense migration from rural areas to urban areas, leading to the abandonment of cultivated lands and their gradual forestation over time. This coincides with the increase in forest areas and decrease in agriculture class in our study. At the same time, this situation also explains the increase observed in the settlement class (Table 5). Additionally, Castillo et al. (2018) and Ettehadi et al. (2022) have emphasised that the abandonment of agricultural lands and the decrease

in rural populations are significant issues worldwide. In fact, the results of his research indicate that between 2015 and 2030, around 11% of agricultural land in the European Union will be at high potential risk of abandonment. Rodríguez-Soler et al. (2020) emphasised that the decrease in rural population significantly affects both demographics and land use. The data from the Turkish Statistical Institute (TUIK) indicates that in Turkey, approximately 35.1% of the population resided in villages and small towns in the year 2000, whereas the current figure shows that only 7.7% reside in rural areas. Again, TUIK data shows that the agricultural areas of our country have decreased by 8% in the last 20 years (TUIK 2020). Bayar (2018) conducted a study where it was observed that although agricultural lands increased due to various reasons such as the introduction of agricultural tractors between 1949 and 1980, there has been a tendency to decrease in agricultural lands especially after 1980. All this information supports that the increase in forest areas can be attributed to migration from rural to urban areas. Another significant factor contributing to the increase in forested areas is the success of the forestry and afforestation activities carried out by the Directorate General of Forestry (GDF) in line with its mission and objectives from the past to the present (GDF 2022). Especially after 2006, in line with its forestry mission, the Directorate General of Forestry has accelerated afforestation and rehabilitation efforts, which it continues to pursue to this day. According to the 2020 report by the Food and Agriculture Organization of the United Nations (FAO), Turkey ranked 6th among the top 10 countries with the highest annual net forest gain during the period of 2010-2020 (FAO 2020; Kaptan 2021). This situation supports both the afforestation efforts by the Directorate General of Forestry and the observation in our study that the rate of land change was faster from 2002 to 2012 compared to 2012-2022. All these approaches additionally support the increase in settlement areas and the finding from intensity analysis that the increase in settlement targets the agriculture class.

Another variable in the study is the water class. It is observed that the water class decreased by 63% during the 20 years of change (Table 5). It is considered that the most influential factor in the change in the water class in the study area is the effects of global climate change. Because the study area experiences annual rainfall amounts that are not evenly distributed throughout the year but occur in sudden and torrential forms. This situation makes it difficult for rainfall to be captured by forests and other vegetation or surface areas and infiltrate to replenish groundwater. Consequently, water sources such as rivers, lakes, and reservoirs cannot be replenished, and rainwater is transported to the seas through surface runoff. The closest and most significant evidence of this situation is the flood disaster that occurred in the study area in 2021. It was reported that on the day of the flood disaster, 240 kilograms of rainfall per square meter fell within 24 hours (TMS, 2021). Aksoy (2023) in a study titled "Flood Risk Analysis with AHP and the Role of Forests in Natural Flood Management: A Case Study from the North of Turkey" observed that land use patterns have the highest impact on flood disaster prediction. In a study conducted by Çiçek and Duman (2017), it was found that in the northern regions of our country, except for summer, there is an increasing trend in rainfall, and it occurs suddenly. Zhang et al. (2016) stated that LULC changes in ecosystems reduce infiltration capacity, thereby indicating an increase in surface runoff and depletion of groundwater. All this shows that freshwater ecosystems are under threat in our country and that it is urgent to develop the necessary measures and policies. It has been emphasised that freshwater ecosystems are one of the most threatened ecosystems on the planet, facing pressures from both human and environmental factors (Kalacska et al. 2017). Hua (2017) stated that river water quality is adversely affected by rapid urbanisation. This situation also supports the notion in our study that the increase in the settlement class targets the decrease in the water class. The results of a study conducted by Saddique et al. (2020) have shown that LULC changes are one of the primary drivers of hydrological changes in the watershed. Additionally, they emphasised that LULC change is a complex pressure source threatening the sustainability and management of water resources. The future scenarios for the study area indicate an increase in forest and settlement areas, while water and agricultural areas are expected to decrease. Some studies have exhibited results similar to ours (Bovida-Portugal et al. 2016; Rimal et al. 2018; Aydın & Eker 2022). Another study conducted by TUIK indicates that Turkey's total population will exceed 100 million in the 2040s (TUIK 2017). This situation also supports the trend observed in our results, indicating an increase in future settlement areas and a decrease in water and agricultural areas. The increase in forest areas will play a positive role in mitigating global climate change. However, specific and proactive measures need to be taken to address the increase in settlement areas and the decrease in agricultural and water areas. The results of the study have shown that it provides important information for forecasters, policy makers, and forest managers now and for future planning.

Conclusions

Intensity analysis provided an opportunity to examine variation across categories for the study area and helped to explain the reasons behind the variation. Forest areas were seen to increase from 2002 to 2022. The overall rate of land change in the study area was faster in the 2002-2012 time period. It was observed that the successful forestry activities carried out by the state as of 2006 and the migration from rural to urban areas in the region had a common effect on this rapid change. Increasing forest areas are the result of afforestation efforts and the forestation of agricultural lands left vacant due to migration. Declining populations have not only contributed to reforestation but have also reduced social pressure on existing forest areas, slowing forest degradation considerably.

The most striking result for the study area is the decrease in mixed forest areas over the years. It is known that mixed forests provide great advantages, especially in terms of biodiversity, forest fires, forest pests, forest products, services, and functions. For this reason, in technical forestry activities such as rejuvenation and maintenance to be carried out in mixed forest areas, it is essential to choose the most accurate calendar and the most appropriate techniques by the characteristics of the species. Many reasons are thought to be responsible for the decline of related stand establishments. One of them is that the benefits and functions that local people expect from forests have changed over time. Another one can be defined as the change in expectations of the timber needs of the country. Finally, errors in forestry works that can be made possible and fires occurring in the current period time are seen as possible. In light of the decline in mixed forest, the greatest measure to be taken to improve this situation is to carry out afforestation activities in the form of mixed forests. It is also important to take the necessary measures against diminishing agricultural land to secure a sustainable food supply. For this reason, decision-makers and policy-makers in terms of both forestry and agriculture should determine their decisions and policies most accurately, starting from the local level to the regions and from the regions to the whole country. For this reason, LULC changes should be addressed with analyses that can provide more detailed information such as intensity analysis instead of classical land change matrices, and focus on the causes and consequences of the changes.

Overall, the results of this study showed that the integration of RS, GIS, and simulation models can be used to monitor, predict, map, and report changes in LULC. İntensity analysis contributes to the interpretation of the speed of changes in LULC over time periods, the gross losses and gains of each category, and how losses and gains are realised across categories subject to transition. The integration of RS, GIS, and simulation models can contribute to the effective planning and management of natural resources such as forests, the regulation of agricultural policies, understanding the drivers of LULC changes, taking necessary measures in advance, and thus making better decisions within the scope of sustainable development.

Competing interests

The author declares that they have no competing interests.

Acknowledgements

I would like to thank the General Directorate of Forestry for providing data on forest type maps during the research process. I would also like to thank Assoc. Prof. Dr. Sinan Kaptan for his support in research analyses.

References

Abino, A.C., Kim, S.Y., Jang, M.N., Lee, Y.J., & Chung, J.S. (2015). Assessing land use and land cover of the Marikina sub-watershed, Philippines. *Forest Science and Technology*, *11*(2), 65-75. https://doi.org/10.1080/21580103.2014.957353

Achmad, A., Hasyim, S., Dahlan, B., & Aulia, D.N. (2015). Modeling of urban growth in tsunami-prone city using logistic regression: Analysis of Banda Aceh, Indonesia. *Applied Geography, 62,* 237-246. https://doi.org/10.1016/j.apgeog.2015.05.001

Agarwal, C., Green, G.M., Grove, J.M., Evans, T.P., & Schweik, C.M. (2002). A review and assessment of land-use change models: dynamics of space, time, and human choice. [General Technical Report NE-297]. Newton Square, PA, USA: Department of Agriculture, Forest Service, Northeastern Research Station. 61 p. https://doi.org/10.2737/NE-GTR-297

Aksoy, H. (2023). Flood risk analysis with AHP and the role of forests in natural flood management: A case study from the north of Türkiye. *Kastamonu University Journal of Forestry Faculty*, 23(3), 282-297. https://doi.org/10.17475/kastorman.1394958

Aksoy, H., & Kaptan, S. (2021). Monitoring of land use/land cover changes using GIS and CA-Markov modelling techniques: A study in Northern Turkey. *Environmental Monitoring and Assessment*, *193*(8), 507. https://doi.org/10.1007/s10661-021-09281-x

Aksoy, H., & Kaptan, S. (2022). Simulation of future forest and land use/cover changes (2019-2039) using the cellular automata-Markov model. *Geocarto International, 37*(4), 1183-1202. https://doi.org/10.1080/10106049.2020.1778102

Aldwaik, S.Z., & Pontius Jr, R.G. (2012). Intensity analysis to unify measurements of size and stationarity of land changes by interval, category, and transition. *Landscape and Urban Planning*, *106*(1), 103-114. https://doi.org/10.1016/j.landurbplan.2012.02.010

Alipbeki, O., Alipbekova, C., Sterenharz, A., Toleubekova, Z., Aliyev, M., Mineyev, N., & Amangaliyev, K. (2020). A spatiotemporal assessment of land use and land cover changes in peri-urban areas: A case study of Arshaly District, Kazakhstan. *Sustainability*, *12*(4): 1556. https://doi.org/10.3390/su12041556

Almirón, N.E., do Pico, G.M.V., Cosacov, A., Paredes, E.N., Dobladez, G.A.R., & Neffa, V. G.S. (2022). The geography of Aspidosperma quebracho-blanco vulnerability, an emblematic species of the South American Gran Chaco. *Forest Ecology and Management, 523*: 120503. https://doi.org/10.1016/j.foreco.2022.120503

Anteneh, Y., Stellmacher, T., Zeleke, G., Mekuria, W., & Gebremariam, E. (2018). Dynamics of land change: insights from a three-level intensity analysis of the Legedadie-Dire catchments. Ethiopia. *Environmental Monitoring and Assessment*, *190*(5): 309. https://doi.org/10.1007/s10661-018-6688-1

Aydın, A., & Eker, R. (2022). Future land use/land cover scenarios considering natural hazards using Dyna-CLUE in Uzungöl Nature Conservation Area (Trabzon-NE Türkiye). *Natural Hazards, 114*(3), 2683-2707. https://doi.org/10.1007/s11069-022-05485-7

Basse, R.M., Omrani, H., Charif, O., Gerber, P., & Bódis, K. (2014). Land use changes modelling using advanced methods: Cellular automata and artificial neural networks. The spatial and explicit representation of land cover dynamics at the cross-border region scale. *Applied Geography, 53*, 160-171.

https://doi.org/10.1016/j.apgeog.2014.06.016

Bayar, R. (2018). Arazi Kullanimi Acisindan Türkiye'de Tarim Alanlarinin Degisimi, In terms of land use change in agricultural areas in Turkey. *Coğrafi Bilimler Dergisi CBD, 16*(2), 187-200. https://doi.org/10.2139/ssrn.3400349

Beroho, M., Briak, H., Cherif, E.K., Boulahfa, I., Ouallali, A., Mrabet, R., Kebede, F., Bernardino, A., & Aboumaria, K. (2023). Future scenarios of land use/land cover (LULC) based on a CA-Markov simulation model: case of a mediterranean watershed in Morocco. *Remote Sensing, 15*(4): 1162. https://doi.org/10.3390/rs15041162

Bewket, W., & Abebe, S. (2013). Land-use and land-cover change and its environmental implications in a tropical highland watershed, Ethiopia. *International Journal of Environmental Studies, 70*(1), 126-139. https://doi.org/10.1080/00207233.2012.755765

Bovida-Portugal, I., Rocha, J., & Ferreira, C.C. (2016). Exploring the impacts of future tourism development on land use/cover changes. *Applied Geography, 77*, 82-91. https://doi.org/10.1016/j.apgeog.2016.10.009

Cammerer, H., Thieken, A.H., & Verburg, P.H. (2013). Spatio-temporal dynamics in the flood exposure due to land use changes in the Alpine Lech Valley in Tyrol (Austria). *Natural Hazards, 68*, 1243-1270. https://doi.org/10.1007/s11069-012-0280-8

Castillo, C.P., Kavalov, B., Diogo, V., Jacobs-Crisioni, C., e Silva, F.B., & Lavalle, C. (2018). Agricultural land abandonment in the EU within 2015-2030. JRC Research Reports JRC113718, Joint Research Centre.

Congalton, R.G., & Green, K. (2019). Assessing the accuracy of remotely sensed data: principles and practices. Third Edition, Boca Raton, CRC press, 348 p. https://doi.org/10.1201/9780429052729

Çiçek, İ., & Duman, N. (2017). Seasonal and annual precipitation trends in Turkey. *Carpathian Journal of Earth and Environmental Sciences, 10*(2), 77-84.

Daba, M.H., & You, S. (2022). Quantitatively assessing the future land-use/land-cover changes and their driving factors in the upper stream of the Awash River based on the CA-Markov model and their implications for water resources management. *Sustainability, 14(*3): 1538. https://doi.org/10.3390/su14031538

Das, B., Bordoloi, R., Deka, S., Paul, A., Pandey, P.K., Singha, L.B., Tripathi, O.P, Mishra, B.P., & Mishra, M. (2021). Above ground biomass carbon assessment using field, satellite data and model based integrated approach to predict the carbon sequestration potential of major land use sector of Arunachal Himalaya, India. *Carbon Management, 12*(2), 201-214. https://doi.org/10.1080/17583004.2021.1899753

Deep, S., & Saklani, A. (2014). Urban sprawl modelling using cellular automata. *The Egyptian Journal of Remote Sensing and Space Science, 17*(2), 179-187. https://doi.org/10.1016/j.ejrs.2014.07.001

Dewan, A.M., & Yamaguchi, Y. (2009). Land use and land cover change in Greater Dhaka, Bangladesh: Using remote sensing to promote sustainable urbanization. *Applied Geography, 29*(3), 390-401. https://doi.org/10.1016/j.apgeog.2008.12.005

Dong, L., Wang, W., Ma, M., Kong, J., & Veroustraete, F. (2009). The change of land cover and land use and its impact factors in upriver key regions of the Yellow River. *International Journal of Remote Sensing, 30*(5), 1251-1265. https://doi.org/10.1080/01431160802468248

Dubovyk, O., Sliuzas, R., & Flacke, J. (2011). Spatio-temporal modelling of informal settlement development in Sancaktepe district, Istanbul, Turkey. *ISPRS Journal of Photogrammetry and Remote Sensing, 66*(2), 235-246. https://doi.org/10.1016/j.isprsjprs.2010.10.002

Ettehadi Osgouei, P., Sertel, E., & Kabadayı, M.E. (2022). Integrated usage of historical geospatial data and modern satellite images reveal long-term land use/cover changes in Bursa/Turkey, 1858-2020. *Scientific Reports, 12*(1): 9077. https://doi.org/10.1038/s41598-022-11396-1

FAO (2020). Global Forest Resources Assessment 2020 - Key findings. Rome.

Gasirabo, A., Xi, C., Hamad, B.R., & Edovia, U.D. (2023). A CA-Markov-based simulation and prediction of LULC changes over the Nyabarongo River Basin, Rwanda. *Land, 12*(9): 1788. https://doi.org/10.3390/land12091788

GDF (2022). Web sitesi. Ormancılık istatistikleri, https://web.ogm.gov.tr/ekutuphane/

Ghosh, J., & Porchelvan, P. (2017). Remote sensing and GIS technique enable to assess and predict land-use changes in Vellore district, Tamil Nadu, India. *IJAER, 12*(12), 3474-3482.

Guan, D., Gao, W., Watari, K., & Fukahori, H. (2008). Land use change of Kitakyushu based on landscape ecology and Markov model. *Journal of Geographical Sciences, 18*(4), 455-468. https://doi.org/10.1007/s11442-008-0455-0

Günlü, A. (2021). Comparison of different classification approaches for land cover classification using multispectral and fusion satellite data: a case study in Ören Forest Planning Unit. *Journal of Bartin Faculty of Forestry, 23*(1), 306-322. https://doi.org/10.24011/barofd.882471

Halmy, M.W.A., Gessler, P.E., Hicke, J.A., & Salem, B.B. (2015). Land use/land cover change detection and prediction in the north-western coastal desert of Egypt using Markov-CA. *Applied Geography, 63*, 101-112. https://doi.org/10.1016/j.apgeog.2015.06.015

Hasan, S., Shi, W., Zhu, X., Abbas, S., & Khan, H.U.A. (2020). Future simulation of land use changes in rapidly urbanizing South China based on land change modeler and remote sensing data. *Sustainability, 12*(11): 4350. https://doi.org/10.3390/su12114350

Hermhuk, S., Chaiyes, A., Thinkampheang, S., Danrad, N., & Marod, D. (2020). Land use and above-ground biomass changes in a mountain ecosystem, northern Thailand. *Journal of Forestry Research, 31*, 1733-1742. https://doi.org/10.1007/s11676-019-00924-x

Hishe, S., Bewket, W., Nyssen, J., & Lyimo, J. (2020). Analysing past land use land cover change and CA-Markov-based future modelling in the Middle Suluh Valley, Northern Ethiopia. *Geocarto International, 35*(3), 225-255. https://doi.org/10.1080/10106049.2018.1516241

Houghton, R.A., House, J.I., Pongratz, J., Van Der Werf, G.R., Defries, R.S., Hansen, M.C., Le Quéré, C., & Ramankutty, N. (2012). Carbon emissions from land use and land-cover change. *Biogeosciences, 9*(12), 5125-5142. https://doi.org/10.5194/bg-9-5125-2012

Hua, A.K. (2017). Land use land cover changes in detection of water quality: a study based on remote sensing and multivariate statistics. *Journal of Environmental and Public Health*, 2017: 7515130. https://doi.org/10.1155/2017/7515130

Huang, C., Yang, H., Li, Y., Zou, J., Zhang, Y., Chen, X., Mi, Y., & Zhang, M. (2015). Investigating changes in land use cover and associated environmental parameters in Taihu Lake in recent decades using remote sensing and geochemistry. *PLoS One, 10*(4): e0120319. https://doi.org/10.1371/journal.pone.0120319

Huang, J., Pontius Jr, R.G., Li, Q., Zhang, Y. (2012). Use of intensity analysis to link patterns with processes of land change from 1986 to 2007 in a coastal watershed of southeast China. *Applied Geography, 34*, 371-384. https://doi.org/10.1016/j.apgeog.2012.01.001

Huang, W., Liu, H., Luan, Q., Jiang, Q., Liu, J., & Liu, H. (2008). Detection and prediction of land use change in Beijing based on remote sensing and GIS. *The International Archives of the Photogrammetry, Remote Sensing and Spatial Information Sciences*, *37*(6), 75-82.

Huang, Y., Yang, B., Wang, M., Liu, B., & Yang, X. (2020). Analysis of the future land cover change in Beijing using CA-Markov chain model. *Environmental Earth Sciences,79*(2), 1-12. https://doi.org/10.1007/s12665-019-8785-z

Isik, S., Kalin, L., Schoonover, J.E., Srivastava, P., & Lockaby, B.G. (2013). Modeling effects of changing land use/cover on daily streamflow: an artificial neural network and curve number based hybrid approach. *Journal of Hydrology*, *485*, 103-112. https://doi.org/10.1016/j.jhydrol.2012.08.032

Jana, A., Jat, M.K., Saxena, A., & Choudhary, M. (2022). Prediction of land use land cover changes of a river basin using the CA-Markov model. *Geocarto International, 37*(26), 14127-14147. https://doi.org/10.1080/10106049.2022.2086634

John, J., Bindu, G., Srimuruganandam, B., Wadhwa, A., & Rajan, P. (2020). Land use/land cover and land surface temperature analysis in Wayanad district, India, using satellite imagery. *Annals of GIS, 26*(4), 343-360. https://doi.org/10.1080/19475683.2020.1733662

Kadioğullari, A.İ., Sayin, M.A., Çelik, D.A., Borucu, S., Çil, B., & Bulut, S. (2014). Analysing land cover changes for understanding of forest dynamics using temporal forest management plans. *Environmental Monitoring and Assessment*, *186*(4), 2089-2110. https://doi.org/10.1007/s10661-013-3520-9

Kafi, K.M., Shafri, H.Z.M., & Shariff, A.B.M. (2014). An analysis of LULC change detection using remotely sensed data; A Case study of Bauchi City. *IOP Conference Series: Earth and Environmental Science*, Volume 20, 7th IGRSM International Remote Sensing & GIS Conference and Exhibition 22–23 April 2014, Kuala Lumpur, Malaysia. https://iopscience.iop.org/article/10.1088/1755-1315/20/1/012056

Kalacska, M., Arroyo-Mora, J.P., Lucanus, O., & Kishe-Machumu, M.A. (2017). Land cover, land use, and climate change impacts on endemic cichlid habitats in northern Tanzania. *Remote Sensing, 9*(6): 623. https://doi.org/10.3390/rs9060623

Kaptan, S. (2021). Changes in forest areas and land cover and their causes using intensity analysis: the case of Alabarda forest planning unit. *Environmental Monitoring and Assessment, 193*: 387. https://doi.org/10.1007/s10661-021-09089-9

Karimi, H., Jafarnezhad, J., Khaledi, J., & Ahmadi, P. (2018). Monitoring and prediction of land use/land cover changes using CA-Markov model: a case study of Ravansar County in Iran. *Arabian Journal of Geosciences, 11*(19), 1-9. https://doi.org/10.1007/s12517-018-3940-5

Khan, M.M.H., Bryceson, I., Kolivras, K.N., Faruque, F., Rahman, M.M., & Haque, U. (2015). Natural disasters and land-use/land-cover change in the southwest coastal areas of Bangladesh. *Regional Environmental Change, 15*, 241-250. https://doi.org/10.1007/s10113-014-0642-8

Khwarahm, N.R., Qader, S., Ararat, K., & Fadhil Al-Quraishi, A.M. (2021). Predicting and mapping land cover/land use changes in Erbil/Iraq using CA-Markov synergy model. *Earth Science Informatics, 14*(1), 393-406. https://doi.org/10.1007/s12145-020-00541-x

Kulkarni, A.D., & Lowe, B. (2016). Random forest algorithm for land cover classification. *International Journal on Recent and Innovation Trends in Computing and Communication, 4*(3), 58-63.

Kumar, K.S., Kumari, K.P., & Bhaskar P.U. (2016). Application of Markov chain & cellular automata based model for prediction of urban transitions. *2016 International Conference on Electrical, Electronics, and Optimization Techniques,* 4007-4012. https://doi.org/10.1109/ICEEOT.2016.7755466

Li, X., Zhou, W., & Ouyang, Z. (2013). Forty years of urban expansion in Beijing: What is the relative importance of physical, socioeconomic, and neighbourhood factors? *Applied Geography, 38*, 1-10. https://doi.org/10.1016/j.apgeog.2012.11.004

Liu, X., Li, Y., Shen, J., Fu, X., Xiao, R., & Wu, J. (2014). Landscape pattern changes at a catchment scale: a case study in the upper Jinjing river catchment in subtropical central China from 1933 to 2005. *Landscape and Ecological Engineering, 10*, 263-276. https://doi.org/10.1007/s11355-013-0221-z

López-Moreno, J.I., Zabalza, J., Vicente-Serrano, S.M., Revuelto, J., Gilaberte, M., Azorin-Molina, C., Morán-Tejeda, E., García-Ruiz, J.M., & Tague, C. (2014). Impact of climate and land use change on water availability and reservoir management: Scenarios in the Upper Aragón River, Spanish Pyrenees. *Science of The Total Environment, 493,* 1222-1231. https://doi.org/10.1016/j.scitotenv.2013.09.031

Mallupattu, P.K., & Sreenivasula Reddy, J.R. (2013). Analysis of land use/land cover changes using remote sensing data and GIS at an Urban Area, Tirupati, India. *The Scientific World Journal*, 2013: 268623. https://doi.org/10.1155/2013/268623

Mathewos, M., Lencha, S.M., & Tsegaye, M. (2022). Land use and land cover change assessment and future predictions in the Matenchose Watershed, Rift Valley Basin, using CA-Markov simulation. *Land, 11*(10): 1632. https://doi.org/10.3390/land11101632

Mayes, M., Marin-Spiotta, E., Szymanski, L., Erdoğan, M.A., Ozdoğan, M., & Clayton, M. (2014). Soil type mediates effects of land use on soil carbon and nitrogen in the Konya Basin, Turkey. *Geoderma, 232*, 517-527. https://doi.org/10.1016/j.geoderma.2014.06.002

Mengistu, D.A., & Salami, A.T. (2007). Application of remote sensing and GIS inland use/land cover mapping and change detection in a part of south-western Nigeria. *African Journal of Environmental Science and Technology, 1*(5), 99-109.

Moniruzzaman, M., Thakur, P.K., Kumar, P., Ashraful Alam, M., Garg, V., Rousta, I., & Olafsson, H. (2020). Decadal urban land use/land cover changes and its impact on surface runoff potential for the Dhaka City and surroundings using remote sensing. *Remote Sensing, 13*(1): 83. https://doi.org/10.3390/rs13010083

Nasiri, V., Darvishsefat, A.A., Rafiee, R., Shirvany, A., & Hemat, M.A. (2019). Land use change modelling through an integrated multi-layer perceptron neural network and Markov chain analysis (case study: Arasbaran region, Iran). *Journal of Forestry Research*, *30*, 943-957. https://doi.org/10.1007/s11676-018-0659-9

Nouri, J., Gharagozlou, A., Arjmandi, R., Faryadi, S., & Adl, M. (2014). Predicting urban land use changes using a CA-Markov model. *Arabian Journal for Science and Engineering*, *39*, 5565-5573. https://doi.org/10.1007/s13369-014-1119-2

Parker, D.C., Manson, S.M., Janssen, M.A., Hoffmann, M.J., & Deadman, P. (2003). Multi-agent systems for the simulation of land-use and land-cover change: a review. *Annals of the association of American Geographers, 93*(2), 314-337. https://doi.org/10.1111/1467-8306.9302004

Patekar, P.R., & Unhale, P.L. (2013). Remote Sensing and GIS application in change detection study using Multi Temporal Satellite. *International Journal of Advanced Remote Sensing and GIS, 2*(1), 374-378. http://technical.cloud-journals.com/index.php/IJARSG/article/view/Tech-181

Pellikka, P.K.E., Heikinheimo, V., Hietanen, J., Schäfer, E., Siljander, M., & Heiskanen, J. (2018). Impact of land cover change on aboveground carbon stocks in Afromontane landscape in Kenya. *Applied Geography, 94*, 178-189. https://doi.org/10.1016/j.apgeog.2018.03.017

Peralta-Rivero, C., Contreras Servín, C., Galindo Mendoza, M.G., Algara Siller, M., & Mas Caussef, J.F. (2014). Deforestation rates in the Mexican Huasteca region (1976-2011). *Journal de Ciencia y Tecnologia Agraria, 3*(1), 1-20.

Qiang, Y., & Lam, N.S. (2015). Modeling land use and land cover changes in a vulnerable coastal region using artificial neural networks and cellular automata. *Environmental Monitoring and Assessment, 187*, 1-16. https://doi.org/10.1007/s10661-015-4298-8

Rimal, B., Sharma, R., Kunwar, R., Keshtkar, H., Stork, N. E., Rijal, S., Rahman, S.A., & Baral, H. (2019). Effects of land use and land cover change on ecosystem services in the Koshi River Basin, Eastern Nepal. *Ecosystem Services, 38*, 100963. https://doi.org/10.1016/j.ecoser.2019.100963

Rimal, B., Zhang, L., Keshtkar, H., Haack, B.N., Rijal, S., & Zhang, P. (2018). Land use/land cover dynamics and modelling of urban land expansion by the integration of cellular automata and Markov chain. *ISPRS International Journal of Geo-Information, 7*(4), 154. https://doi.org/10.3390/ijgi7040154

Rodríguez-Soler, R., Uribe-Toril, J., & Valenciano, J.D.P. (2020). Worldwide trends in the scientific production on rural depopulation, a bibliometric analysis using bibliometrix R-tool. *Land Use Policy, 97*, 104787. https://doi.org/10.1016/j.landusepol.2020.104787

Rubio, L., Rodríguez-Freire, M., Mateo-Sánchez, M.C., Estreguil, C., & Saura, S. (2012). Sustaining forest landscape connectivity under different land cover change scenarios. *Forest Systems, 21*(2), 223-235. https://doi.org/10.5424/fs/2012212-02568

Saddique, N., Mahmood, T., & Bernhofer, C. (2020). Quantifying the impacts of land use/land cover change on the water balance in the afforested River Basin, Pakistan. *Environmental Earth Sciences, 79*(19), 448. https://doi.org/10.1007/s12665-020-09206-w

Sahana, J.M., Jennifer, J., & Vanmathy, S. (2016). Land use/land cover change prediction using clue-s model. *IJEST, 6*(3), 176-182.

Santer, B.D., Wigley, T.M.L., Boyle, J.S., Gaffen, D.J., Hnilo, J.J., Nychka, D., Parker, D.E. & Taylor, K.E. (2000). Statistical significance of trends and trend differences in layer-average atmospheric temperature time series. *Journal of Geophysical Research: Atmospheres, 105*(D6), 7337-7356. https://doi.org/10.1029/1999JD901105

Santillan, J., Makinano, M., & Paringit, E. (2011). Integrated Landsat image analysis and hydrologic modelling to detect impacts of 25-year land-cover change on surface runoff in a Philippine watershed. *Remote Sensing, 3*(6), 1067-1087. https://doi.org/10.3390/rs3061067

Singh, B., Venkatramanan, V., & Deshmukh, B. (2022). Monitoring of land use land cover dynamics and prediction of urban growth using Land Change Modeler in Delhi and its environs, India. *Environmental Science and Pollution Research, 29*(47), 71534-71554. https://doi.org/10.1007/s11356-022-20900-z

Snedecor, G., & Cochran, W. (1969). Statistical methods 6th ed. Ames, IA, USA: The Iowa State University Press.

TMS (2021). Turkish State Meteorological Service, https://www.mgm.gov.tr/eng/forecast-cities.aspx

TUIK (2017). Turkey in Statistics 2017. https://biruni.tuik.gov.tr/yayin/views/visitorpages/index.Zul Accessed 28 November 2020.

TUIK (2020). Population of province/district centers and towns/villages by years and sex, 1927-2019. http://www.tuik.gov.tr/PreIstatistikTablo.do?istab_id=1587. Accessed 28 November 2020.

USGS (2022). United States Geological Survey, Landsat Missions, Landsat 8. https://www.usgs.gov/ Accessed 06 November 2020.

Wang, R., & Murayama, Y. (2017). Change of land use/cover in Tianjin city based on the Markov and cellular automata models. *ISPRS International Journal of Geo-Information, 6*(5): 150. https://doi.org/10.3390/ijgi6050150

Weslati, O., Bouaziz, S., & Sarbeji, M.M. (2023). Modelling and assessing the spatiotemporal changes to future land use change scenarios using remote sensing and CA-Markov model in the Mellegue catchment. *Journal of the Indian Society of Remote Sensing, 51*(1), 9-29. https://doi.org/10.1007/s12524-022-01618-4

Xie, Q., & Sun, Q. (2021). Monitoring the spatial variation of aerosol optical depth and its correlation with land use/land cover in Wuhan, China: a perspective of urban planning. *International Journal of Environmental Research and Public Health, 18*(3): 1132. https://doi.org/10.3390/ijerph18031132

Yacouby, R., & Axman, D. (2020). Probabilistic extension of precision, recall, and f1 score for more thorough evaluation of classification models. In Proceedings of the first workshop on evaluation and comparison of NLP systems, pages 79-91, Online. Association for Computational Linguistics, (pp. 79-91). https://aclanthology.org/2020.eval4nlp-1.9.pdf https://doi.org/10.18653/v1/2020.eval4nlp-1.9

Yagoub, M.M., & Al Bizreh, A.A. (2014). Prediction of land cover change using Markov and cellular automata models: case of Al-Ain, UAE, 1992-2030. *Journal of the Indian Society of Remote Sensing, 42*, 665-671. https://doi.org/10.1007/s12524-013-0353-5

Yilmaz, Y.A., Sen, O.L., & Turuncoglu, U.U. (2019). Modeling the hydroclimatic effects of local land use and land cover changes on the water budget in the upper Euphrates-Tigris basin. *Journal of Hydrology, 576*, 596-609. https://doi.org/10.1016/j.jhydrol.2019.06.074

Zadbagher, E., Becek, K. & Berberoglu, S. (2018). Modeling land use/land cover change using remote sensing and geographic information systems: case study of the Seyhan Basin, Turkey. *Environmental Monitoring and Assessment, 190*: 494. https://doi.org/10.1007/s10661-018-6877-y

Zhang, L., Nan, Z., Yu, W., & Ge, Y. (2016). Hydrological responses to land-use change scenarios under constant and changed climatic conditions. *Environmental Management, 57*, 412-431. https://doi.org/10.1007/s00267-015-0620-z

Zheng, H.W., Shen, G.Q., Wang, H., & Hong, J. (2015). Simulating land use change in urban renewal areas: a case study in Hong Kong. *Habitat International, 46*, 23-34. https://doi.org/10.1016/j.habitatint.2014.10.008